



## Master Thesis

Masterarbeit zur Erlangung des akademischen Grades eines Diplom Ingenieurs der Studienrichtung  
Pharmaceutical Engineering an der Technischen Universität Graz

# Immobilization of a Model Enzyme on Si(111) Surfaces via UV-lithography

Richard Rittenschober

Advisor:  
DI Dr. techn. Heidrun Gruber-Wölfler



Institute for Process and Particle Engineering  
Research Group Pharmaceutical Engineering

Graz, May 2012

Deutsche Fassung:  
Beschluss der Curricula-Kommission für Bachelor-, Master- und Diplomstudien vom 10.11.2008  
Genehmigung des Senates am 1.12.2008

## EIDESSTATTLICHE ERKLÄRUNG

Ich erkläre an Eides statt, dass ich die vorliegende Arbeit selbstständig verfasst, andere als die angegebenen Quellen/Hilfsmittel nicht benutzt, und die den benutzten Quellen wörtlich und inhaltlich entnommenen Stellen als solche kenntlich gemacht habe.

Graz, am .....

.....  
(Unterschrift)

Englische Fassung:

## STATUTORY DECLARATION

I declare that I have authored this thesis independently, that I have not used other than the declared sources / resources, and that I have explicitly marked all material which has been quoted either literally or by content from the used sources.

.....  
(Date)

.....  
(Signature)

## Danksagung

An dieser Stelle möchte ich mich recht herzlich bei allen Personen bedanken die mich beim Verfassen dieser Arbeit unterstützt haben, aber auch bei all jenen die mir in der gesamten Studienzeit mit Rat und Tat zur Seite gestanden haben.

An erster Stelle möchte ich mich bei Prof. Dr. Johannes Kinast und bei Dr. Heidi Gruber-Wölfler bedanken die es mit ermöglicht haben meine Masterarbeit am Institut für Prozess und Partikeltechnik zu verfassen. Bei Dr. Heidi Gruber-Wölfler möchte ich mich speziell bedanken, die mich während der gesamten Zeit am Institut durch ihre persönliche und kompetente Betreuung unterstützt hat.

Ich möchte mich auch bei allen Kollegen am Institut bedanken, insbesondere bei Christoph Neubauer der mir die goniometrischen Messungen ermöglichte, sowie bei DI Georg Lichtenegger, der mir in der praktischen Einarbeitung in das Thema sehr behilflich war.

Für die fachliche Zusammenarbeit möchte ich mich bei Prof. Dr. Gübitz bedanken, der auch die Enzyme zur Verfügung stellte.

Große Unterstützung zur Bewältigung des Studiums fand ich stets bei Freunden, Kollegen, und meiner Familie. Ich darf mich glücklich schätzen, dass ich Eltern habe auf die ich mich immer verlassen kann, dafür kann ich ihnen nicht genug danken.

Bei allen Freunden aus Graz aber auch in meiner Heimat bedanke ich mich für gemeinsames Wohnen und so manche heitere Tage und Nächte, vielen Dank.

Ich hoffe es folgen viele weitere.

## Kurzfassung

Die vorliegende Master Arbeit befasst sich mit der kovalenten Immobilisierung von Enzymen auf Wasserstoff-terminierten Silizium (111) Oberflächen mit Hilfe von Photolithographie. Silizium wurde als Basis gewählt, da durch einfache Nass-ätzmethoden quasi atomar flache Si-H Oberflächen erzeugt werden können. Auf diesen Flächen können sich Linker-Moleküle in selbstorganisierten molekularen Monoschichten anordnen. Die Bindung der Enzyme an die Silizium Oberfläche erfolgte durch den Einsatz von bi-funktionellen Linker-Molekülen. Bei den Linker-Molekülen handelt es sich um langkettige 1-Alkene mit terminalen funktionellen Gruppen zur kovalenten Enzymbindung. Die C-C Doppelbindung des Linker-Moleküls bindet an die Si- Oberfläche durch UV-induzierte Hydrosilylierung unter Ausbildung einer Si-C Bindung. Unter Einsatz einer Photomaske kann durch die UV-induzierte Reaktion eine ortsspezifische Funktionalisierung der Si-Oberfläche realisiert werden. Die Enzymbindung erfolgte anhand zwei verschiedener Systemen, die verglichen wurden. Einerseits wurde eine terminale Epoxid-gruppe genutzt, andererseits eine Carboxyl-gruppe, die durch Einsatz von *N*-Hydroxysuccinimid (NHS) / 1-Ethyl-3-(3-dimethylaminopropyl)carbodiimid (EDC) zu einem aktivierten Ester umgewandelt wurde. Als Linker-Moleküle wurden 1,2-Epoxy-9-decen (2-(7-Octen-1-yl)oxiran) und 10-Undecylensäure verwendet. Als Modelenzym diente eine Laccase von dem Pilz *Trametes Hirsuta*. Der Grund für die Wahl der Laccase ist eine relativ hohe Stabilität des Enzyms und der Umstand, dass die Umsatzbestimmung des Substrats Dimethoxyphenol (DMP) UV/Vis spektroskopisch verfolgt werden kann. Die Silizium Proben wurden nach den einzelnen Reaktionsschritten durch Kontaktwinkelmessungen (WCA), Fourier-Transformations-Infrarotspektroskopie (FTIR) und Röntgenphotoelektronenspektroskopie (XPS) charakterisiert. Weiters wurde die Aktivität und die Stabilität des immobilisierten Enzyms gemessen und mit den theoretischen Maximalwerten verglichen. Die Ergebnisse zeigen, dass sich die beiden relativ simplen Immobilisierungsmöglichkeiten gut zur kovalenten Bindung von Enzymen auf Silizium Oberflächen eignen.

## Abstract

This master thesis deals with the covalent immobilization of enzymes on hydrogen-terminated silicon (111) surfaces via photolithography. Silicon was used as immobilization substrate because silicon crystals offer the possibility to produce virtually atomically flat Si-H surfaces through simple chemical wet etching methods. Linker molecules form self-assembled monolayers (SAMs) on these surfaces, which leads to highly ordered functionalities. The ligation of the enzyme to the silicon surface is carried out by means of bi-functional linker molecules. The linker molecules are long-chain alkenes with terminal functional groups for binding to enzymes. The carbon-carbon double bond of the linker is attached to the silicon surface through UV-induced hydrosilylation under formation of a silicon-carbon bond. The commitment of a photo mask allows the realization of site-specific functionalization on the silicon surface. The binding to the enzyme is performed by two different linker systems, which have been compared. One system was the attachment via a terminal epoxide group. The second system was a carboxylic group, which was transformed into an activated ester by means of *N*-hydroxysuccinimide and 1-ethyl-3-(3-dimethylaminopropyl)carbodiimide (EDC). The used linkers were 1,2-epoxy-9-decene (2-(7-octen-1-yl)oxirane) and 10-undecylenic acid. To verify successful enzyme immobilization, a laccase from *trametes hirsuta* (fungi), was used as a model enzyme for activity tests. The reason for the choice of this enzyme is the high stability and the fact that enzyme assays, based on the conversion of dimethoxyphenol, can be monitored by UV/Vis spectroscopy. The functionalized silicon samples were characterized by water contact angle measurements (WCA), Fourier transform infrared spectroscopy (FTIR) and X-ray photoelectron spectroscopy (XPS) after the single reaction steps. Additionally, all samples were tested in enzyme assays for their activity and their stability. Both linking methods are relatively simple and showed to be suitable methods for covalent attachment of enzymes on silicon.

## Table of content

1. Introduction.....	1
2. Background.....	3
2.1. Silicon Characteristics .....	3
2.2. Cleaning.....	5
2.3. Etching .....	6
2.3.1. Removal of Oxide Layer .....	6
2.3.2. Etching of Bulk Silicon .....	9
2.3.3. Etching with Acidic Fluoride Solutions .....	13
2.3.4. Etching in Basic Fluoride Solutions.....	15
2.3.5. Etch-pit Formation .....	17
2.3.6. Summary of Etching Parameters:.....	18
2.4. Binding of Molecules on Si Wafers, Formation of SAMs .....	19
2.5. Immobilization of Enzymes.....	23
2.5.1. Non-covalent Protein Adsorption .....	24
2.5.2. Classical Covalent Immobilization .....	24
2.5.3. Site-specific Immobilization .....	26
2.6. Catalysis.....	28
2.6.1. Homogeneous Catalysis.....	29
2.6.2. Heterogeneous Catalysis.....	29
2.6.3. Phase-transfer Catalysis.....	31
2.6.4. Biocataylsis.....	31
2.6.5. Kinetics and Activity .....	32
3. Process, Results & Discussion .....	34
3.1. Cutting.....	34
3.2. Cleaning.....	35
3.3. Etching .....	36
3.4. Immobilization of Linker Molecule .....	36
3.4.1. Linker with Terminal Activated Ester Group.....	37
3.4.2. Linker with Terminal Epoxy Group.....	41
3.5. Activation of Linker Molecule.....	41

3.6. Enzyme Immobilization Step .....	42
3.7. Water Contact Angle Measurement .....	43
3.8. FTIR Measurement .....	46
3.9. Enzyme Activity.....	49
3.9.1. Optimization of Immobilization pH Value .....	52
3.9.2. Calculation of Maximum Immobilization.....	55
3.9.3. Activity Measurement Without Stirring .....	56
3.9.4. Ex-situ Activity Measurements.....	58
3.9.5. Stability Test .....	59
3.10. X-ray Photoelectron Spectroscopy (XPS) .....	61
4. Summary & Outlook.....	64
5. Experimental Details.....	66
5.1. Silicon Wafer Specifications .....	66
5.2. UV Source.....	66
5.3. Water Contact Angle Measurement .....	66
5.4. FTIR Measurement .....	66
5.5. UV/Vis Measurement .....	66
5.6. XPS Measurement .....	67
5.7. Used Chemicals .....	67

---

## List of Figures

Figure 1-1: Schematic approach .....	2
Figure 2-1: Silicon tetrahedrons .....	3
Figure 2-2: Top view of silicon tetrahedrons.....	3
Figure 2-3: Silicon crystal in diamond cubic structure .....	4
Figure 2-4: Fluoride species at different pH values .....	7
Figure 2-5: SiO <sub>2</sub> etch in fluoride solution .....	7
Figure 2-6: SiO <sub>2</sub> etch in alkaline solution.....	8
Figure 2-7: Schematic reaction of bulk etch through back-bond polarization .....	8
Figure 2-8: Step etch mechanism.....	10
Figure 2-9: Etch rate at different sites .....	10
Figure 2-10: Silicon with kink site .....	11
Figure 2-11: Silicon with point site.....	11
Figure 2-12: Miscut of wafer and etched steps.....	12
Figure 2-13: Etching mechanism of alkaline etch.....	13
Figure 2-14: Bulk silicon etch at open circuit potential.....	14
Figure 2-15: Electrochemical etch .....	14
Figure 2-16: Etching via chemical mechanism .....	16
Figure 2-17: Hydrosilylation reaction .....	19
Figure 2-18: Reaction mechanism of radical-induced hydrosilylation.....	20
Figure 2-19: Top view on a Si(111) surface .....	22
Figure 2-20: Immobilization of linker.....	22
Figure 2-21: Classical covalent Immobilization.....	25
Figure 2-22: Reaction scheme of a catalyzed reaction.....	29
Figure 2-23: Energy diagram of catalyzed and uncatalyzed reaction .....	29
Figure 2-24: Transport processes in heterogeneous catalysis .....	30
Figure 2-25: Langmuir-Hinshelwood mechanism .....	30
Figure 2-26: Eley-Rideal mechanism .....	30
Figure 3-1: Silicon (111) crystal with silicon double layer .....	35
Figure 3-2: Functionalization of Si(111)-H surface with undecenoic acid (UA).....	38
Figure 3-3: Lithographic box covered with fused silica window .....	39
Figure 3-4: Side view lithographic box.....	39
Figure 3-5: Pattern on silicon wafer (A); 1951 USAF resolution test chart (B).....	40

Figure 3-6: Functionalization of Si(111)-H surface with epoxy linker .....	41
Figure 3-7: Activation of terminal carboxylic acid with NHS/EDC .....	42
Figure 3-8: Reaction vessel for linker activation .....	42
Figure 3-9: Immobilization of protein on activated ester surface (NHS-UA) .....	43
Figure 3-10: Immobilization of protein on epoxide terminated surface .....	43
Figure 3-11: Water contact angle $\theta$ .....	44
Figure 3-12: Water contact angles .....	44
Figure 3-13: FTIR transmission spectrum of a Si(111)-H wafer .....	47
Figure 3-14: FTIR transmission spectrum Si-wafer .....	48
Figure 3-15: Schematic reaction of the used enzyme with diphenol.....	50
Figure 3-16: Laccase from <i>trametes hirsuta</i> .....	50
Figure 3-17: Enzymatic conversion of dimethoxyphenol to diphenoquinone .....	52
Figure 3-18: Enzyme assay .....	53
Figure 3-19: UV/Vis calibration measurement .....	54
Figure 3-20: Activity measurement without stirring .....	56
Figure 3-21: Enzymatic activity measurement with shaking .....	58
Figure 3-22: Stability Test.....	59
Figure 3-23: XPS spectrum of wafer with immobilized undecenoic acid linker .....	61
Figure 3-24: XPS spectrum of wafer with immobilized epoxid linker .....	62
Figure 3-25: XPS spectrum of wafer with immobilized enzyme via NHS-UA-linker...	63

## List of tables

Table 2-1: Examples for enzymes and their catalytic efficiency .....	33
Table 3-1: Water contact angle of oxide layer .....	44
Table 3-2: Visual activity test.....	51
Table 3-3: Enzymatic activity of enzyme-UA-wafer without stirring .....	57
Table 3-4: Stability test; wafer with activated ester linker .....	60
Table 3-5: Stability test; wafer with epoxide linker .....	60
Table 3-6: Results X-ray photoelectron spectroscopy measurement .....	61
Table 3-7: Elemental compositions of linkers and enzyme.....	62

---

## List of abbreviations

[E]	Enzyme concentration
[S]	Substrate concentration
A	Frequency factor in Arrhenius equation
APTES	3-Aminopropyltriethoxysilane
ATR	Attenuated total reflectance
BHF	Buffered hydrogen fluoride solution
c	Concentration in mol * L <sup>-1</sup>
Cz	Czochralski
d <sub>DL</sub>	Distance silicon double layer in (111) direction
DNA	Deoxyribonucleic acid
e <sup>-</sup>	Electron
E <sub>A</sub>	Activation energy
EC	Enzyme classification
EDC	1-Ethyl-3-(3-dimethylaminopropyl)carbodiimide
EPL	Expressed protein ligation
eV	Electron Volt
FTIR	Fourier transform infrared spectroscopy
h	Hours
H/W	Height/Width
h <sup>+</sup>	Hole
IC	Integrated circuits
K	Rate constant
k <sub>Cat</sub>	Turnover frequency
kDa	Kilo Dalton, 1000 g/mol
K <sub>M</sub>	Michaelis constant
M	Molar (mol * L <sup>-1</sup> )
min	Minutes
M <sub>w</sub>	Molecular Weight
NHS	<i>N</i> -Hydrosuccinimide (1-Hydroxy-2,5-pyrrolidinedione)
PTFE	Polytetrafluoroethylene
R	Universal gas constant
RCA	Radio cooperation of America

## List of abbreviations

---

RT	Room temperature
SAM	Self-assembled monolayer
SC	Standard cleaning solution
S <sub>N</sub>	Nucleophilic substitution
T	Temperature
t-RNA	Transfer ribonucleic acid
U	Activity unit in $\mu\text{mol}$ per minute
UA	Undecenoic acid
UHV	Ultra high vacuum
USAF	United States Air Force
UV	Ultra violet light
Vis	Visible light
V <sub>Max</sub>	Maximal reaction velocity at substrate saturation
WCA	Water contact angle
wt%	Weight percent
XPS	X-ray photoelectron spectroscopy
$\delta+$ / $\delta-$	Positive/ negative partial charge
$\Theta$	Water contact angle

## 1. Introduction

The attachment of biomolecules to carrier systems is an important topic in many scientific and technical areas. The applications range from micro-arrays for medical and pharmaceutical development <sup>[1]</sup> to heterogeneous biocatalysts for the production of base chemicals and pharmaceuticals.<sup>[2][3][4]</sup> The used biomolecules are mainly proteins and DNA, which are generally immobilized via a linker. The linker is a bifunctional molecule which attaches to the support on one side and on the other side to the biomolecule, either through physisorption or through a covalent bond. The advantage of a covalent bond is the higher binding energy and it is therefore more stable. In most cases the covalent bond formation is irreversible and leaching of the adsorbed molecule is thus avoided.

Today the focus is on the development of biosensors <sup>[5][6][7][8]</sup>, micro-reactors <sup>[9]</sup>, DNA and protein microarrays.<sup>[10]</sup> Therefore, flat substrates are preferred. Many papers deal with the immobilization of biomolecules on glass slides <sup>[11]</sup> or on silicon substrates with attached oxide layers.<sup>[12][13][7]</sup> In these cases, a bond is established between the silanol surface and a trialkoxysilane linker by a silyl-ether formation. The disadvantage of this amorphous surface is the hardly controllable density of Si-OH groups and a higher inhomogeneity of the layer.<sup>[14]</sup>

In the last decade particular attention was paid to the attachment of biomolecules to silicon crystals. Silicon offers remarkable properties because of the semi conducting nature and the anisotropic crystal structure. Electron transfer from the Si substrate to the biomolecule could offer new ways for sensing and biocomputing.<sup>[15]</sup> Moreover, the expertise in silicon microprocessing for integrated circuits can be used for fabrication of micro structured biochips.<sup>[16][17][18]</sup>

One important point for the use of silicon is the possibility to create virtually atomically flat hydrogen-terminated surfaces through simple chemical wet etching.<sup>[33][51][19][20]</sup> These surfaces allow attaching linker molecules in a highly ordered manner to so called self-assembled monolayers (SAMs).<sup>[21]</sup> The most established reaction to bind linker to the surface is the hydrosilylation.

The hydrosilylation is the Si-C bond formation between a terminal alkene or alkyne with the Si-H surface.<sup>[22][27]</sup> The advantage of the hydrosilylation is the formation of a

stable bond and the fact that the reaction can be initiated by three ways (thermally, radical-induced and UV-induced). To initiate the reaction by UV light is an elegant way to produce patterns on wafer.<sup>[23]</sup> The attachment of the alkene linkers only takes place at illuminated spots, which can be realized by the use of a photo mask.

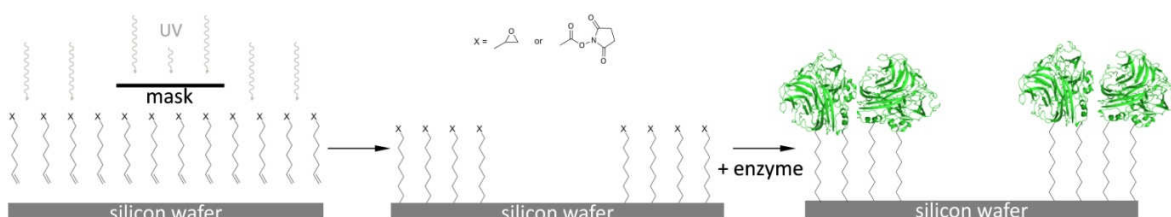


**Figure 1-1: Schematic approach of enzyme immobilization**

In general the linker molecule is a long-chain alkene or alkyne molecule. The advantage of a carbon based linker is the versatile chemistry, which allows the use of a large variety of terminal end groups for immobilization purposes.

The goal of this thesis is to immobilize a model enzyme on a flat Si(111) surface (Figure 1-1) with high surface coverage without reducing the activity of the enzyme. Therefore two enzyme immobilization methods should be tested, one through an activated ester group and the second through a terminal epoxide (oxirane) group. These two linkers should be compared and they should demonstrate being feasible molecules for immobilization of enzymes.

In particular the goals of the work are:

- ❖ Production and characterization of flat Si-H surfaces on silicon wafers
- ❖ Attachment of the linker molecules and production of patterns
- ❖ Immobilization of an enzyme
- ❖ Surface analysis
- ❖ Activity test of enzyme

Subsequently, efforts should be made to produce multifunctional heterogeneous catalysts by attaching different biological and inorganic catalysts on defined spots on the silicon wafer.

## 2. Background

### 2.1. Silicon Characteristics

Silicon is the second most abundant element in the earth crust and appears mainly in silicate compounds.<sup>[24]</sup> Elemental silicon can be produced in a single crystal form up to dimensions greater than 10 inches in diameter and several meters in length.<sup>[25]</sup> Prime grade silicon substrates can be purchased at relative low price, because high purity silicon is the base for the production of integrated circuits. Over the last decades the industry achieved a lot of experience in producing high purity single crystal silicon wafers.

In most cases, silicon is tetravalent and forms tetrahedral geometrics, as shown in Figure 2-1 and Figure 2-2. Elemental silicon crystallizes in diamond cubic structure (Figure 2-3). The most silicon crystals for commercial use are grown in the  $[111]$  or in the  $[100]$  direction and are produced in dislocation-free processes. In the process all the dislocations are grown out of the crystal into a neck with a smaller diameter, before the crystal is grown in the desired diameter.<sup>[25]</sup>

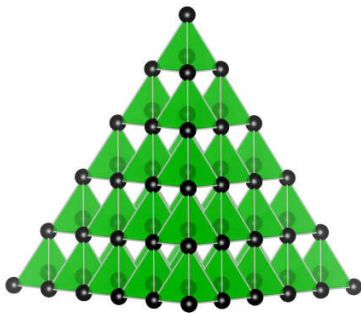


Figure 2-1: Silicon tetrahedrons  
 $[111]$  = upward direction <sup>[25]</sup>

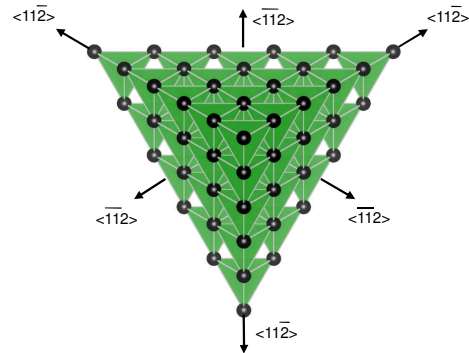


Figure 2-2: Top view of silicon tetrahedrons <sup>[25]</sup>

In ambient atmosphere Silicon forms a thin  $\text{SiO}_2$  layer, which acts as a diffusion barrier with passivating effects. The Si-O bond is more stable than the C-O bond through partial double bonding, which explains the high chemical stability. The free electron pair from the oxygen is overlapping with the free d-orbitals from silicon.<sup>[26]</sup> The oxide layer can be removed chemically or thermally.<sup>[27]</sup>

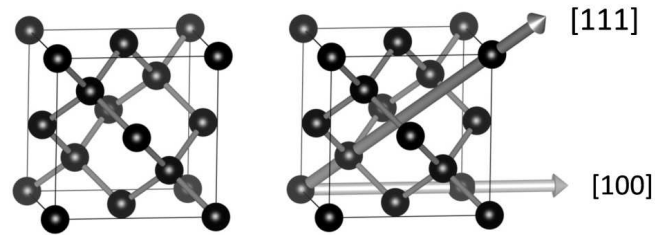


Figure 2-3: Silicon crystal in diamond cubic structure, with vectors (right) <sup>[25]</sup>

Silicon is in the 14th group of the periodic table and belongs to the semiconducting elements. The most silicon substrates for electrical purposes are doped with elements from the neighboring groups in the periodic table.

The purpose of doping is the increase of the electrical conductivity. The gap between the valence band and the conducting band is 1.107 eV at room temperature. This gap can be reduced through doping with group thirteen or group fifteen elements. Doping elements from the fifteenth group, like phosphorus and arsenic, are acting as donor atoms. They are adding extra valence electrons. These electrons can act as negative charge carriers. Such semiconductors are called n-type semiconductors. Doping elements from the thirteenth group, like boron and aluminum are acting as acceptor atoms. They only have three valence electrons and create electronic holes in the silicon lattice. These holes act as movable charge carriers and these semiconductors are called p-type semiconductors.

## 2.2. Cleaning

The cleaning of silicon wafers is a well explored process, since cleaning methods are important in IC manufacturing.

For the cleaning two wet cleaning procedures are known, cleaning with the “RCA standard clean”, developed by the Radio Cooperation of America <sup>[28]</sup> or the cleaning with the so called “piranha”-solution.<sup>[29]</sup>

The “RCA standard clean” is composed of two cleaning steps with two cleaning solutions. The “Standard Cleaning 1” solution (SC1) consists of 5 volume parts deionized water, 1 part concentrated ammonium hydroxide solution and 1 part hydrogen peroxide (30 wt% in H<sub>2</sub>O). In the “Standard Cleaning 2” solution (SC2) the ammonium hydroxide is replaced by concentrated hydrochloric acid. The cleaning in SC1 is for removing organic contaminations of the wafers. In addition some metals like copper and nickel form complexes with ammonium hydroxide and get removed.

The second step is the immersion in “SC2” solution, for removing alkali ions and cations like Al<sup>3+</sup> and Fe<sup>3+</sup>.

The piranha solution is a 3:1 mixture of concentrated sulfuric acid and hydrogen peroxide (30 wt% in H<sub>2</sub>O). The piranha solution is a strong oxidizing solution and is favorable for heavily contaminated wafers, e.g. for recycling of functionalized wafers or to remove photoresist layers. The disadvantage of this method is the possibility of contaminating the surface with sulfur. So it is recommendable to combine the piranha solution cleaning and the SC 2 cleaning.<sup>[28]</sup>

After cleaning, the silicon surface is covered with a silicon oxide layer.

## 2.3. Etching

Etching can be divided into two steps:

- ❖ Removal of the oxide layer
- ❖ Isotropical etch of the bulk silicon

The reason for etching is the creation of atomically flat silicon surfaces with moderate reactivity for further surface reactions.

Two main etching solutions are known for wet chemical etching of silicon and silicon compounds, hydrofluoric acid solutions and alkaline solutions. To gain optimal etching results alkaline fluoride solutions can be used. The alkaline fluoride etchant has a combined etching mechanism, which features the benefits of the alkaline and the hydrofluoric acid etch.<sup>[51][30][19]</sup>

### 2.3.1. Removal of Oxide Layer

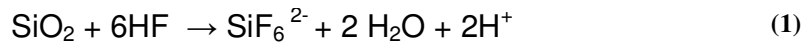
When bare silicon is in contact with atmospheric oxygen or aqueous solutions, it immediately builds a native oxide layer. This oxide layer can grow to a thickness of several angstroms.<sup>[29][30]</sup> The oxide layer acts as a passivation layer and inhibits further oxidation of bulk silicon.

For immobilization purposes, the reactivity of the silicon dioxide layer is in an acceptable range and many papers deal with this topic.<sup>[7][12][13]</sup> One used linker molecule is APTES ((3-aminopropyl)-triethoxysilane) which is bound to the silanol groups through Si-O-Si bonds. This thesis doesn't deal with the immobilization via APTES because the immobilization on bare silicon substrates is advantageous. The silicon oxide layer, especially the native grown one, shows surface inhomogeneity and surface roughness. Furthermore, the layer is non-crystalline and acts as electrical isolator.<sup>[31][29]</sup>

The reason for the use of bare silicon crystals for immobilization purposes is the high homogeneity of the surface, which allows highly packed surface substitution. Furthermore, the direct Si-C bond, between the silicon and a carbon based linker, is a less polar binding. Additionally, no electrical isolation layer is between the bulk silicon and the substituent.

The removal of the native oxide layer is carried out preferably with fluoride solutions. Two different fluoride species are responsible for it, as described in equation (1) and equation (2).<sup>[30]</sup>

Etching Mechanisms:



The lower the pH, the more important is reaction (1). At higher or neutral pH the reaction (2) is the main reaction (Figure 2-4).<sup>[30][31]</sup> For the removal of the oxide layer low pH and high HF concentrations are preferable for high reaction rates.

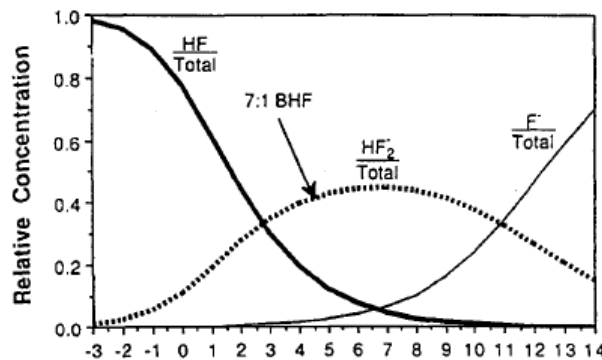


Figure 2-4: Fluoride species at different pH values, figure from MONK et al.<sup>[31]</sup>

The fluoride ion attacks the Si-O-Si bonds as shown in Figure 2-5. This reaction progresses until the whole silicon oxide layer is dissolved and the bulk silicon is reached. A similar mechanism is valid for the attack by OH<sup>-</sup> in alkaline solutions, as shown in Figure 2-6.

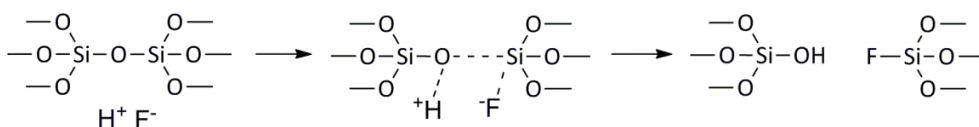


Figure 2-5: SiO<sub>2</sub> etch in fluoride solution<sup>[31]</sup>

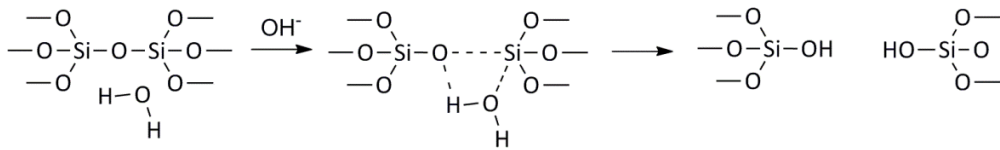


Figure 2-6: SiO<sub>2</sub> etch in alkaline solution<sup>[31]</sup>

After removal of the silicon oxide layer, the underlying bulk silicon is H-terminated, which is equal for both etching mechanisms.

*BURROWS* et al.<sup>[32]</sup> discovered that etching in fluoride solutions is leading to H-termination. Initially they expected a fluoride termination after etching. The reason for the assumption is the fact that the Si-F bond is thermodynamically favored. In their IR-studies, they reported the absence of fluoride ions on the etched surfaces.<sup>[32][33][34]</sup> This results from the high polarity of the Si-F bond. Through the polarity of the Si-F bond the Si-Si back-bond is also polarized. The polarization is weakening the bond to the bulk silicon, which allows the attack of water molecules (Figure 2-7). The formed surface dangling bond is then terminated by hydrogen. The mechanism of back-bond polarization is also valid for etching with OH<sup>-</sup>.

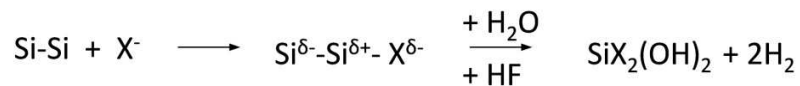


Figure 2-7: Schematic reaction of bulk etch through back-bond polarization

The first step is the rate determining step. The dissolution step is very fast, so only H-terminated silicon surface atoms can be detected on the etched wafer.

The termination of silicon by hydrogen provides the outlined advantages of moderate surface reactivity, which allows handling in atmosphere for short periods, but still provides the possibility for further chemical modifications. Further reactions on the H-terminated should be carried out in inert atmosphere to avoid oxidative degradation.

The oxidative degradation is caused by interplay between humidity and atmospheric oxygen and forms a native oxide layer.<sup>[35]</sup> The initiation step of the oxidation is not site-specific, but leads to oxygen island grow.<sup>[36][37]</sup>

There are also other ways to remove the oxide layer, e.g. ultra-high vacuum (UHV) methods. In the UHV method, the oxide layer is removed thermally under vacuum and a highly reactive Si-Si-double bond is formed and directly reacted, e.g. with alkenes or alkynes. This method needs no precursors, but it is more sensitive against atmospheric oxygen. Samples prepared by UHV methods can only be handled in high purity inert atmosphere or in UHV. The disadvantage of these methods is a higher effort regarding equipment costs.

### **2.3.2. Etching of Bulk Silicon**

The goal of etching bulk silicon is to reduce surface roughness. The basic principle of flattening a surface is anisotropic etching. The crystal structure of silicon possesses the requirements for anisotropic etching due to the anisotropic characteristics of the diamond cubic structure. In addition, the anisotropic etching is particularly dependent on the etching mechanism.

For immobilization purposes a silicon crystal is used with a surface facing [111] direction. In the [111] direction the silicon surface atoms are bound to three bulk silicon atoms. The remaining fourth binding site is perpendicular to the surface and is occupied by a hydrogen atom. That arrangement is very stable and the H-termination is passivating the surface in this direction. Due to the passivation the etching rate of the (111) surface is lower than in all other crystallographic directions. That also means that the etching rates are higher at surface defects, for example at steps. A step is the change to the next crystal layer. These defects are polishing- and cutting defects from wafer manufacturing.<sup>[42]</sup>

The order of etching velocities at different sites is shown in Figure 2-9. The highest etching velocities are given at silicon trihydride sites and all are removed at the beginning of the etching. Silicon atoms at step and kink sites have high etch rates in contrast to silicon monohydrides.

Silicon atoms at step and kink sites are only bond to two bulk silicon atoms and are therefore vulnerable for attacks. The steric hindrance for the attack of the Si-Si-bond is lowered.

That means that whole layers can be erased, starting from steps sites, before the surface is attacked. This is called step flow process. Figure 2-8 shows a schematic illustration of the step flow process.

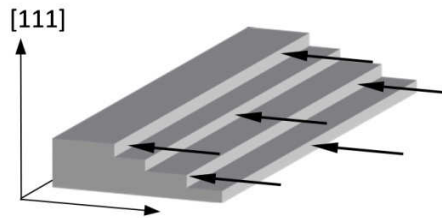


Figure 2-8: Step etch mechanism

The step quality of the flow process depends on the mechanisms of the etchant. That means that the etching mechanism determines the differences in etching velocities for different sites. The higher the differences in etching rates from kink and step sites compared to the [111] direction, the better the step flow process works.<sup>[37][38][20][19]</sup>

Figure 2-9 outlines the reactivity of the different sites on the silicon crystal.

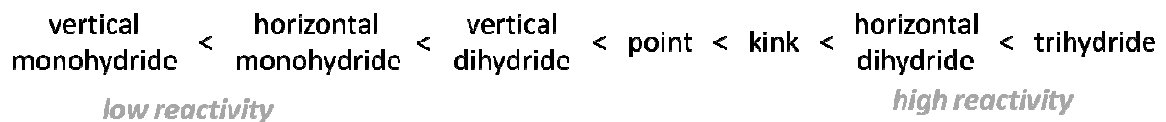


Figure 2-9: Etch rate at different sites<sup>[37]</sup>

Steps are showing either in  $\langle 112 \rangle$  or in  $\langle \bar{1}\bar{1}2 \rangle$  directions. The steps in  $\langle 112 \rangle$  direction are terminated by horizontal monohydrides. When this monohydride-silicon is removed, then it is followed by a trihydride silicon and the next silicon is again a horizontal monohydride. In the  $\langle \bar{1}\bar{1}2 \rangle$  direction the silicon atoms are vertical dihydrides. Is this vertical dihydride-silicon removed, than the next silicon is a horizontal dihydride.

Sites where the  $\langle 112 \rangle$  direction and the  $\langle \bar{1}\bar{1}2 \rangle$  direction are forming an edge are called kinks (Figure 2-10). When two  $\langle 112 \rangle$  directions are forming a shark tooth shape, the sharp end is called a point site (Figure 2-11).<sup>[19][39]</sup>

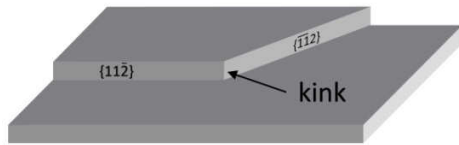


Figure 2-10: Silicon with kink site <sup>[19]</sup>

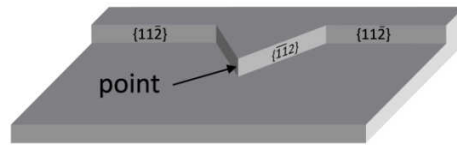


Figure 2-11: Silicon with point site <sup>[19]</sup>

Up to a certain dimension the differences in etching rates allow the production of almost atomically flat surfaces. Still some surface attacks can occur, but the etching rate from kink sites has to be high enough to erase the whole layer before deeper etching spots can occur. Beyond this critical dimension, the surface etching is competing with the step etching and some surface etching spots occur.

To overcome this problem, wafers with off-cut-orientation are used (see Figure 2-12). That means that the wafer is not cut parallel to the (111) plane, but is slightly tilted. The angle can be varied between 0.1 and 3°. The miss-cut creates step sites on the surface of the wafer, where the attack in the  $[1\ 1\ 2]$  and in the  $[\bar{1}\ \bar{1}\ 2]$  direction can occur (see Figure 2-8). Through this procedure terraces with highly homogeneous surfaces are built. Every step is an initiation site for the step flow process and the pitting is suppressed. Pitting is the attack of silicon on terraces.

The characteristics of the terraces depend on the tilt angle and the direction of the tilt angle. The higher the tilt angle the more, but the smaller terraces are built.<sup>[37]</sup> The optimal surface for immobilization is given at the lowest tilt angle where pitting is still sufficiently suppressed.

The direction of the tilt angle affects the shape of the terraces. When the (111) plane is tilted towards the  $[1\ 1\ 2]$  -direction the steps are straight and parallel. When the (111) plane is tilted towards the  $[\bar{1}\ \bar{1}\ 2]$  -direction, steps with “hillocks” are formed.<sup>[40]</sup>

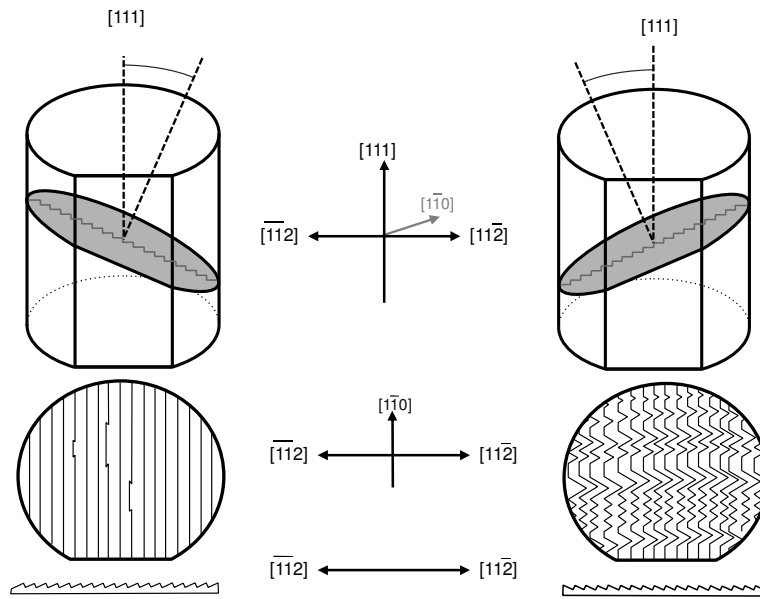


**Figure 2-12: Miscut of wafer and etched steps** <sup>[19]</sup>

The wet chemical etching of silicon with  $\text{OH}^-$  or with  $\text{F}^-$  is quite similar, such as the removal of silicon atoms through back-bond polarization or the H-termination of the bulk silicon. The important difference is the initiation step, which further leads to different structures in the etched product. Wet etching can be used to produce flat surfaces or to produce porous and nano-crystalline porous silicon.

Etching with basic solutions: <sup>[30][41]</sup>



Equation (3) describes the etching reaction of silicon in alkaline solution. The etching mechanism (Figure 2-13) in alkaline solutions is a pure chemical mechanism. Here the electronegative  $\text{OH}^-$  plays a catalytic role and attacks the Si analogous to a  $\text{S}_\text{N}$  reaction. A pentavalent transition state is formed. The produced  $\text{H}^-$  is reacting with water to  $\text{H}_2$  and  $\text{OH}^-$ . <sup>[42]</sup>

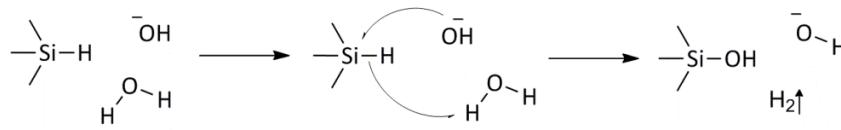


Figure 2-13: Etching mechanism of alkaline etch <sup>[42]</sup>

The produced  $\text{OH}^-$  group on the Si surface is responsible for the Si-Si back-bond polarization.<sup>[43]</sup>

Bases can flatten silicon surfaces up to a certain pH via the step flow mechanism. At very high pH some surface roughness is induced. The high  $\text{OH}^-$  concentration leads to temporary elevated number of OH-groups on the silicon surface. The OH-groups on a surface normally lead to back-bond polarization and a fast dissolution, but when neighboring OH-groups are built, it can lead to a condensation reaction with a resulting oxide. The oxide can be removed again but the etching process is inhomogeneous and flattening is prevented.

Another disadvantage of etching in alkaline solutions is the slow removal of the initial oxide layer on silicon. Compared to fluoride etching, the removal of the passivation oxide layer is 3-4 magnitudes slower.<sup>[44][45]</sup> To obtain good etching results, it is preferable to remove the oxide layer first, by etching in HF.

### 2.3.3. Etching with Acidic Fluoride Solutions

Acidic fluoride solutions, like hydrofluoric acid, are known for their etching properties, especially for silicon oxides. Fluoride solutions are etching the silicon oxide layer and an H-terminated surface is produced. This surface is quite resistant against further chemical attack of HF. Without an applied voltage or illumination the bulk silicon is virtually inert in concentrated HF solutions.

The etching of acidic fluoride solutions is based on an electrochemical mechanism and electronic excitation of the surface is required.<sup>[30][43]</sup>

The initiation plays an important role in the electrochemical mechanism. The initiation with the followed fluoride bond formation is the rate determining step. The silicon-fluoride bond is highly polarized with leads to a Si-Si back-bond polarization. This makes it susceptible to attack.

The electrochemical mechanism is not as site specific as the chemical mechanism. Even if the electrochemical mechanisms attacks more likely at step and kink sites than on terraces, the differences in reaction rates are not high enough to follow the step flow process. The electrochemical mechanism can therefore lead to the formation of porous silicon.

There are three different initiation steps: <sup>[30]</sup>

- ❖ Hole injection
- ❖ Applied voltage
- ❖ Stain etching

The first way to initiate the etching is to form a bulk hole-electron-pair through illumination above band gap and transportation of the hole to the surface. This is described by the *GERISCHER* mechanism <sup>[30]</sup> and is shown in Figure 2-14.

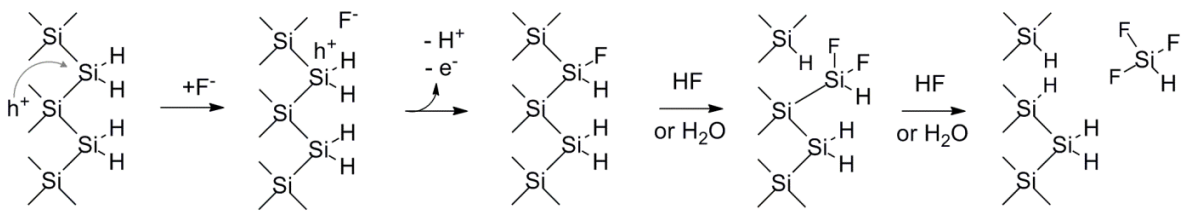


Figure 2-14: Bulk silicon etch at open circuit potential <sup>[46]</sup>

The second way is to apply an anodic bias or to use stain chemicals. The stain etching is an open-circuit reaction where an oxidizing agent is abstracting electrons from the valence band of the silicon, i.e., holes are injected. These holes are mobile electric carriers and when they are located at the surface, they cause breakage of chemical bonds.

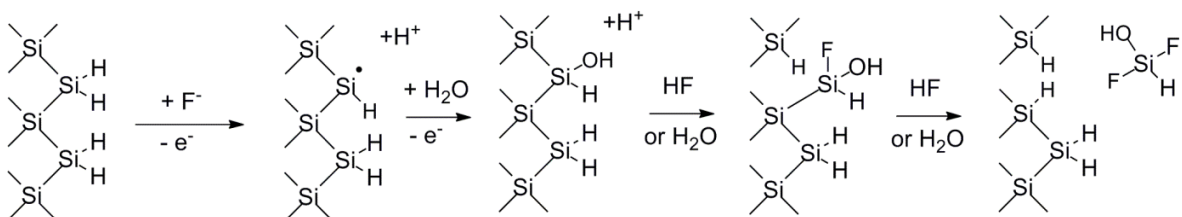


Figure 2-15: Electrochemical etch <sup>[48]</sup>

The etching with applied voltage or with illumination is leading to porous and nano-crystalline porous silicon. The mechanism for the production of nano-crystalline porous silicon is not fully understood but it is proposed to be related to quantum confinement effects.

The silicon is etched to a certain degree, when the structures reach the nanoscale etching stops self because the characteristics of formation and transportation of holes are altered. The holes are transported preferentially to the bottom of the pores, as the walls are passivated through quantum confinement effects. This enables an anisotropic pore growth.

#### **2.3.4. Etching in Basic Fluoride Solutions**

The goal of the basic fluoride etching is to optimize the step flow process.

Etching of silicon in basic fluoride solutions is combining the concepts of basic etch and the HF-etch. *ALLONGUE* et al.<sup>[47]</sup> proposed that the pH of the fluoride solution gives different surface morphologies. They showed that etching with fluoride solutions is underlying two different etching mechanisms, the chemical mechanism like in basic etching and the electrochemical mechanism of acidic fluoride etches. The anisotropic chemical mechanism is dominating already in neutral or slightly basic solutions.<sup>[48]</sup> Even if the main mechanism is the same as for fluoride-free bases, the addition of fluoride advances the step flow process (Figure 2-16).

Fluorides are important to facilitate the dissolution process. Once the chemical initiation took place, the fluoride is able to change against the hydroxide group.<sup>[48]</sup> This leads to increased back-bond polarization.

The building of the silanol group is the rate determining step as no silanol groups are found in IR-measurements. The dissolution step is very fast, so only H-termination is observed.<sup>[30][32]</sup>

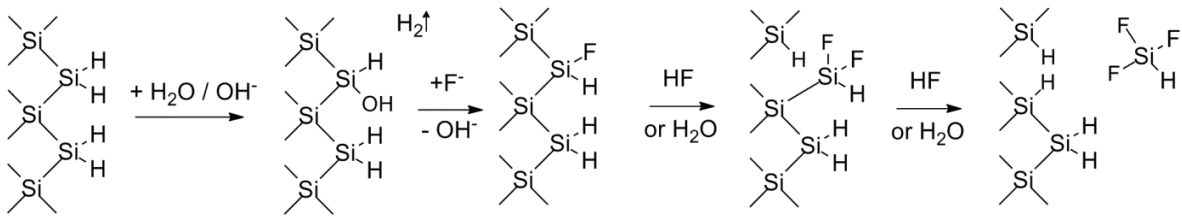


Figure 2-16: Etching via chemical mechanism <sup>[43][51]</sup>

The etching product  $\text{HF}_x\text{Si}(\text{OH})_{3-x}$  is further hydrolyzed and produces another  $\text{H}_2$  molecule (equation 4).<sup>[48][30]</sup>



Another advantage, compared to the purely basic etch, is that the etching proceeds already at neutral to basic pH values. This avoids the problem of silanol group condensation.

In practice, 40% aqueous ammonium fluoride solutions are used for etching with a pH value of 8.<sup>[49][50]</sup>

*ALLONGUE* et al.<sup>[51]</sup> showed another effect which is responsible for the chemical flattening. Their simulations show that the etching rate on kink sites has to be at least 7 magnitudes higher than on terraces, this could not be explained only by steric effects.<sup>[37]</sup> They explain this observation with cathodic protection of the surface. The already subordinated electrochemical process takes preferably place at defect areas, like rough edges or the rough backside of a wafer. These defect areas are acting as sacrificial anode. The electrons which are induced into the valence band are protecting the flat surfaces of the wafer against further electrochemical attack. The protection of the terraces is only given in oxygen free solutions. In air saturated solutions this protection is contra productive as the oxygen-etch-pitting is promoted.

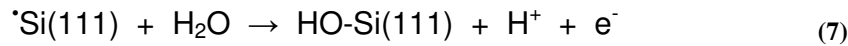
In experiments they showed that the formation of quasi perfect surfaces is possible if only one side is polished. In two side polished wafers they obtained some surface roughness.

After producing defect areas, through scratching with sandpaper, quasi perfectly flat surfaces could be obtained again. There the produced defect areas were acting as sacrificial anode.

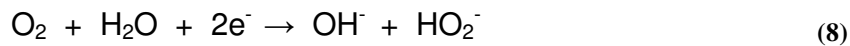
### 2.3.5. Etch-pit Formation

Another critical parameter for wet chemical etching is the absence of dissolved oxygen. The dissolved oxygen is responsible for etch pit formation. Etch pit formation is related to the electrochemical etching mechanism.

The mechanism for the etch-pit formation is not assured yet, but the relation of dissolved oxygen and high etch-pit formation is well established. *WADE* et al.<sup>[47]</sup> proposed the formation of superoxide anion radicals, which attack the Si(111) surface, as described in equation (6).



*ALLONGUE* et al.<sup>[51]</sup> proposed a simple local pH-induced pitching (Equation (8) and (9)). The reaction rate is higher at higher pH. Through the following reaction the pH-value is raised locally.



Etch-pit formation is an isotropic process and is competing with the step flow process. When the etch pit formation is slow, then the pits combine with the etched areas from the step flow process before they can attack the next underlying silicon layers. At faster pit formation, larger pits can be produced and new etching points will be induced, which can grow some bilayers into the surface. The dissolution of the layers is not fast enough anymore to avoid deep etch pits. The pits have a triangular shape where one corner is showing in the  $\langle 112 \rangle$  direction.

The solution to the problem is to remove the dissolved oxygen. Oxygen free etching solutions can be achieved through sparging with argon or to use deoxygenating chemicals like ammonium sulfite. *KATO et al.*<sup>[52]</sup> made series with varying etching times and deoxygenator concentrations and found out that 1% ammonium sulfite solutions and etching in ammonium fluoride (40%) for 10 minutes gave the best results.

### **2.3.6. Summary of Etching Parameters:**

There are some critical key points in the preparation of flat H-Si(111) surfaces: The use of high quality silicon wafers, the cleaning procedure, the etching chemicals and the etching time.<sup>[51]</sup>

The Si substrate has to be a high quality single crystal with very low imperfections of the crystal. The crystal has to be free of dislocations and has to be low doped.

Nowadays substrates in high quality are available with a relative low price.<sup>[37]</sup>

In practice, processes can be carried out in subsequent steps which include the fast isotropic removal of the passivation SiO<sub>2</sub>-layer through concentrated HF solution first and then the bulk etching in basic fluoride solutions.

## 2.4. Binding of Molecules on Si Wafers, Formation of SAMs

The common way to bind active molecules to a silicon crystal is to use linker molecules. These linker molecules are bound on one side to the silicon and on the other side they can be bound to the active molecule via a functional group.

The best option is to use a hydrocarbon chain based linker molecule with a functional end group. The advantage of using an organic linker is the versatile range of different, well established reactions.

The linker is either bound to the silicon first and then to the active molecule, or the other way round. This depends on the chemistry of the functional group. When the functional group can also form a bond to silicon, it can be beneficial to create first the binding between linker and the active molecule.

The reason for using linker molecules is the versatile range of different reactions, as outlined before, but also the protection of the silicon substrate against oxidation and chemical attacks by solvents, acids and bases.

The linker molecules are in a chain form and when they are chemisorbed on crystals they form self-assembled mono-layers (SAMs). The molecule chains in the monolayer are well ordered due to Van der Waals interactions.<sup>[53]</sup>

For immobilization of organic molecules on Si the hydrosilylation reaction is suitable. The hydrosilylation is leading to a Si-C bond, which is thermodynamically and kinetically stable with bond strength of  $369 \text{ kJ mol}^{-1}$  and a low polarity.<sup>[27]</sup>

The hydrosilylation is a radical reaction between H-terminated silicon and an alkene or an alkyne (Figure 2-17).

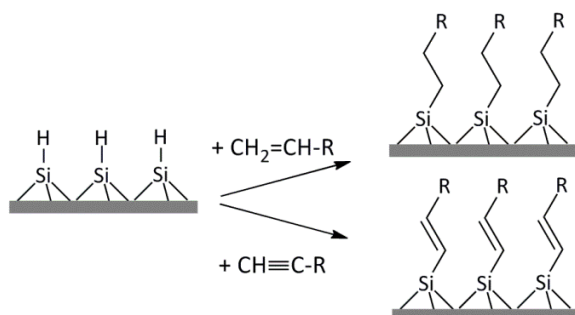
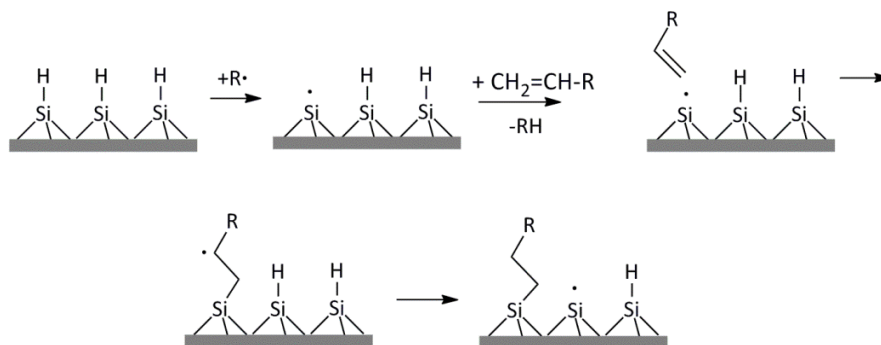


Figure 2-17: Hydrosilylation reaction <sup>[27]</sup>

For the hydrosilylation reaction wet chemical etching is preferable, as the silicon is already H-terminated. A surface hydrogen atom is subtracted by the initiator radical and leaves a surface radical behind. This radical reacts very fast with the olefins by formation of a Si-C bond.<sup>[54]</sup>



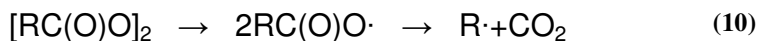
**Figure 2-18: Reaction mechanism of radical-induced hydrosilylation**<sup>[27]</sup>

The abstraction of hydrogen is mainly from neighboring Si atoms but can alternatively be from the allylic position of an unreacted alkene. The generated neighbor Si radical can react again with an alkene and is proceeding in a radical chain reaction mechanism (Figure 2-18). *CICERO* et al. showed in their Monte Carlo simulation that the average number of steps is at 78. This means that the chain reaction stops itself as no neighboring Si-H is available any more. The simulation is based on a process of a self-avoiding random walk on the triangular lattice of the Si(111) face. *CICERO* et al.<sup>[56]</sup> proposed that their simulations are not realistic enough as every neighboring hydrogen atom is giving equal weight. The simulation is not attending to steric effects, which would propose a higher number of steps, or attractive interactions to immobilized linkers, which could lower the number of steps. For immobilization of styrene it was shown that the average number of reaction steps is reduced to about 20 steps.<sup>[55]</sup> Further it could be elaborated that the radical is surface based as no polymerization of styrene was observable.

There are three ways to accomplish the hydrosilylation reaction:

- ❖ radical initiation
- ❖ thermal hydrosilylation
- ❖ photochemical hydrosilylation

A typical radical starter is diacyl peroxide, which produces two alkane radicals under slightly elevated temperatures, as shown in equation (10).



For higher temperatures (>150°C) the hydrosilylation takes place without a radical starter. The Si-H bond is cleaved homolytically and proceeds as the radical initiated reaction (10). The disadvantage of the thermal hydrosilylation is that neat alkenes or concentrated alkene solutions have to be used to achieve a high pack density.

The third way is to illuminate the silicon surface with UV light in alkene solutions. The UV-light is causing the homolytic Si-H bond cleavage and the hydrosilylation reacts again in the same way like the radical initiated. The Si-H has a bond strength of 3.4-3.65 eV, so the threshold for bond cleavage is at 350 nm with 3.5 eV.<sup>[56]</sup> An exception is the white light-induced photochemical hydrosilylation on porous nano-crystalline silicon. There electron-hole formation is responsible for the reaction instead of heterolytic Si-H bond cleavage. The surface localized hole facilitates the nucleophilic attack by an alkene or an alkyne to form a pentavalent state. The hydrogen is then transferred to the positive charged  $\beta$ -carbon atom.<sup>[27]</sup>

Independent of the initiation of the hydrosilylation, a thermodynamical maximal coverage is given. Neighboring substitution of silicon is leading to Van der Waals radii penetration which is unfavorable. Coverage without direct neighbors is given at 33%. On the other side, attractive Van der Waals forces between alky chains are rising at higher coverage. This is leading to equilibrium coverage of 50-55%.<sup>[27][53]</sup> The presence of neighboring silicon substitution is in accordance with the radical chain reaction. The unreacted Si-H bonds stay intact, due to the protection by the monolayer.<sup>[53]</sup> The alkyl chains are approximately 30° tilted to the surface normal (Figure 2-20).

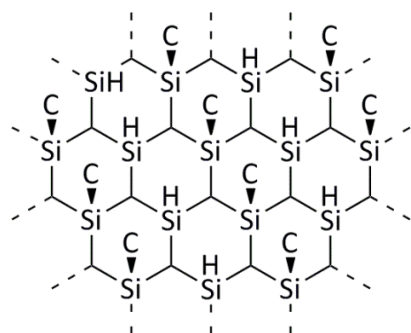


Figure 2-19: Top view on a Si(111) surface <sup>[53]</sup>

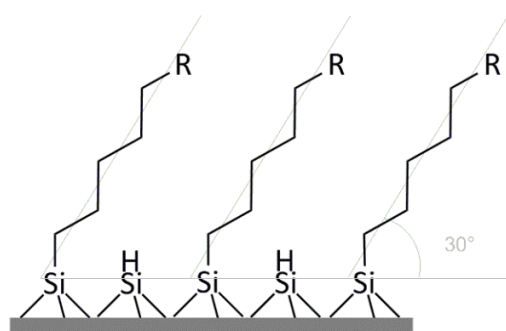


Figure 2-20: Immobilization of linker <sup>[53]</sup>

Figure 2-19 shows a simplified model of the Si(111) surface substitution. The surface bonds are substituted by 50% hydrogen (H) and by 50% alkyl chains (C).

## 2.5. Immobilization of Enzymes

Strategies for immobilization of proteins and enzymes include:

- ❖ Non covalent protein adsorption
- ❖ Classical covalent immobilization
  - NHS-ester functionalized
  - Aldehyde functionalized
  - Epoxide functionalized
  - Maleimide functionalized
- ❖ Site-specific covalent immobilization
  - Staudinger ligation method
  - “Click”-chemistry

The immobilization of proteins is important for different technical applications, for example for protein microarrays for the research and development of new pharmaceuticals <sup>[1][10]</sup>, microarrays for diagnostics, for biosensors <sup>[5][6][7][8]</sup> and for enzymatic micro-reactors.<sup>[9]</sup>

The goal of the immobilization is to prepare surfaces with a high density of intact and active proteins. They should be bound tightly to achieve a high robustness and a good recyclability without leaching out the protein. At best it would be possible to generate homogenous surfaces through specific immobilization of proteins out of cell lysates.

The most used methods are the classical immobilization methods. They are straight forward and applicable to all proteins, but they can generate some issues concerning conformational changes and unspecific orientation. As proteins and enzymes have active centers, unspecific orientation can reduce the accessibility to their active center, which leads to loss of activity. A more recent method is the site-specific covalent immobilization. It is not as straight forward as it is in the case of the classical methods. Mostly these methods are biologically mediated, because a specific region of the protein has to be recognized. These regions can be natural occurring regions or regions that are inserted in post-translational modification or recombination

chemistry. The site-specific immobilization is more complicated, more information about the protein is needed. Additionally some sites of the protein have to be altered with protein engineering methods. The advantage of the method is the high activity through perfect orientation.

### 2.5.1. Non-covalent Protein Adsorption

The non-covalent adsorption is the simplest way to immobilize proteins. The method is based on physical interactions such as adsorption on hydrophobic surfaces (e.g. nitrocellulose membranes or polystyrene microtiter plates) or electrostatic binding on charged surfaces (e.g. polylysine coated slides). The binding method is unspecific which leads also to immobilization of contaminations. Furthermore, there is no control of the packing density, which can lead to steric congestion. The binding forces are weak and reversible, which causes leaching of the protein and in succession to loss of activity. The non-covalent adsorption is inappropriate for devices, which should be robust and recyclable.<sup>[10]</sup>

### 2.5.2. Classical Covalent Immobilization

Proteins have different functional groups like carboxy-, amine- or thiol-groups. In the field of classical covalent immobilization the coupling is based on reactions between the functional groups on the protein and functional groups of linker molecules. The advantage of this method is that no previous modification or labeling of the protein is needed. Furthermore no coupling reagents are needed, which allows mild reaction conditions.<sup>[10]</sup>

With the choice of the linker's functional group, different coupling modes are possible. Some linkers are specific to one functional group, others are reacting with different protein functionalities, but with differential affinities. Both methods have in common that they cannot achieve a site selective binding of proteins with a defined orientation.

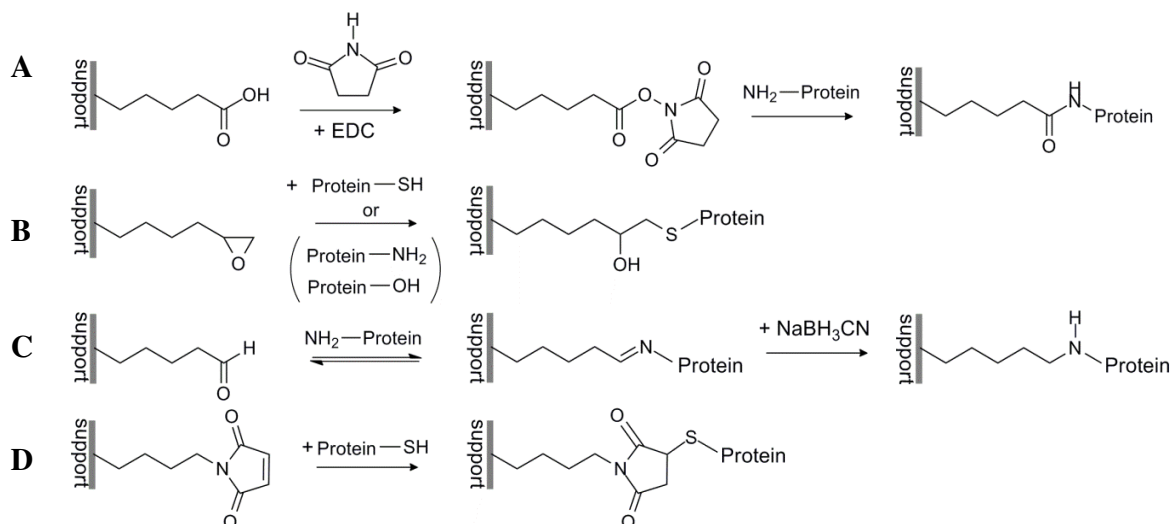


**Figure 2-21: Classical covalent immobilization**  
 activated ester (A), epoxide (B), aldehyde (C) and maleimide (D) <sup>[10]</sup>

For the classical immobilization a wide range of functional linker groups is conceivable. In Figure 2-21 four important ways are illustrated.

Carboxylic acids can form amide bonds with amines when the reaction is assisted by EDC. The disadvantage is that the reaction is very slow and susceptible for hydrolysis, therefore a further step is introduced. The carboxylic acid is first transformed to an active ester (Figure 2-21 A). This is carried out through a reaction between the carboxylic acid and EDC/NHS. The activated NHS ester is relatively stable against hydrolysis compared to other activated esters.<sup>[57]</sup> For the reaction with amines the hydrolysis plays a secondary role as the amidation is faster than the hydrolysis at physiological conditions. Especially at a slightly elevated pH (e.g. pH 8) the amidation reaction kinetics are accelerated more than the kinetics of the hydrolysis.<sup>[58][59]</sup>

The reaction with NHS/EDC is also possible in the opposite direction, to activate the carboxylic group of the protein and to immobilize it on an amine linker. The risk of this reaction is that cross coupling between the proteins can occur.

The advantage of the immobilization by means of an oxirane group is that no activation step is needed (Figure 2-21B).<sup>[81]</sup> The epoxide is reacting with several nucleophiles either under base or acid catalysis. The epoxide is relatively stable against hydrolysis but relatively slow in coupling.<sup>[10][60]</sup>

One approach is to immobilize two different linker molecules, one with the epoxy group and a second one, which binds proteins through physisorption. This linker is responsible to attract the protein which brings the protein in proximity to the epoxide groups. Thereby the covalent immobilization velocity through the epoxide is appreciably elevated.<sup>[61]</sup> In general, epoxides are reacting with thiol-, alcohol-, amine- and carboxyl-groups.

Aldehyde linkers form a reversible bond with exposed amines to give labile imines (Schiff's base). By reducing with sodium cyanoborohydride a secondary amine can be formed. The disadvantage is the need of a further step and the commitment of a reducing chemical.<sup>[10][60]</sup>

At a neutral pH the maleimide groups reacts only with protein-thiols. This means that the multipoint attachment by linker surfaces with maleimide groups is reduced. The disadvantage is that the bond can be hydrolyzed more easily compared to other immobilization methods.<sup>[10]</sup> Linker with maleimide groups offer the possibility to immobilize via a semi-site-specific method. Normally proteins have very few surface exposed cysteine residues, so if there is a single surface exposed cysteine residue you can achieve a site specific binding of the protein. This also allows the modification of proteins through protein engineering to implement a single cysteine amino acid in a natural protein.

### 2.5.3. Site-specific Immobilization

The reaction partners in the site specific immobilization have bioorthogonal functional groups. That means that these groups are not occurring in natural systems, which avoids side reactions with molecules without these groups.<sup>[10]</sup> Furthermore, they should form stable reaction-adducts under mild conditions. There are two important methods described in literature, the Staudinger bond formation<sup>[62][63][64]</sup> and the click chemistry.<sup>[62][65]</sup>

Both methods need two steps, the first step is the insertion of a bioorthogonal group onto the protein. The second step is the actual immobilization step with bond formation between the surface linker group and the protein.

For the Staudinger reaction the peptide has to be tagged with an azide moiety. This azide group is reacting with an immobilized triarylphosphin-group (susceptible to oxidation) to form a nucleophilic iminophosphorane intermediate and further to an amide. In the click chemistry the peptide has to be modified with an alkyne and reacts with an immobilized azide under Cu(I) catalysis to form a triazol-bond. The second step in the Staudinger reaction and click chemistry is a purely chemoselective reaction and fulfills the above mentioned requirements, but the challenging step is the first one. The bioorthogonal group has to be inserted on a specific area in the protein. One possibility is to use the expressed protein ligation (EPL) <sup>[62]</sup> which allows binding peptides with N-terminal cysteine-groups to proteins with alpha-thioesters through transthioesterification, further a spontaneous S-N acyl shift occurs to form a natural peptide bond. The small peptide has to carry the bioorthogonal group (azide- or alkyne-group) or the intermediate thioester reacts with azide substituted hydrazine.<sup>[10][62][66]</sup> The peptide terminated by the alpha-thioester is produced through recombination methods.

A second, promising possibility is to use recombinant proteins with site specific insertion of non-natural amino acids. The non-natural amino acid is translational incorporated through an aminoacylated stop codon suppressor tRNA which is encoded for the UAG stop codon. The tRNA is aminoacylated chemically with the non-natural amino acid. The non-natural amino acid could have an azide or alkyne functional group.<sup>[67]</sup>

There are also other approaches like biologically mediated immobilization methods but they need a lot of prior biological engineering. Examples include Expressed Protein Ligation Fusion Protein Immobilization, enzymatic site selective labeling (post translational methods) and translational insertion of bioorthogonal Tags.<sup>[62]</sup>

To achieve high activity, the site specific immobilization is the optimal way for protein immobilization, but this is only working under certain conditions. The problem is to attach the special group onto the protein, but if this step is managed the actual immobilization step is very specific, which also allows immobilizing out of cell lysates.

## 2.6. Catalysis

More than 90% of chemical processes use catalysts at least in one reaction step.<sup>[68]</sup>

Catalysis is the increase of the reaction rate of a chemical reaction through commitment of a catalyst, without changing the thermodynamic equilibrium. The catalyst is a substance which undergoes a reaction with the educts, under formation of a reaction intermediate. The reaction intermediate features a potential energy which is lower than the activation barrier of the reaction without catalyst. The total activation energy of the catalyzed reaction is lower than the activation energy for uncatalyzed reaction. In other words, the activation barrier is lowered.<sup>[68]</sup>

The activation barrier influences the reaction rate, which is described by the Arrhenius law (Equation (11)). In some cases the initial activation barrier is so high that the reaction is kinetically hindered and no reaction would take place without a catalyst. In these types of reactions the catalyst can also be seen as a reaction starter.

$$k = A * e^{-\frac{E_A}{R*T}} \quad (11)$$

The reaction intermediate is turned into the product under release of the catalyst and the catalyst is ready for the next catalytic circle (Figure 2-22). The catalyst does not undergo any chemical modification and is not consumed during the reaction.

Catalysis can be divided in different categories:

- ❖ Homogeneous catalysis
- ❖ Heterogeneous catalysis
- ❖ Phase transfer catalysis
- ❖ Biocatalysis
- ❖ Photocatalysis
- ❖ Electrochemical catalysis

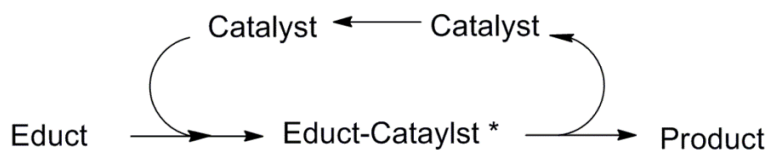


Figure 2-22: Reaction scheme of a catalyzed reaction

### 2.6.1. Homogeneous Catalysis

In homogeneous catalysis the catalyst and the substrates are in the same phase. In the most cases homogeneous catalysis takes place in the liquid or in the gaseous phase. The catalyst is dissolved in the reaction medium. The disadvantage of homogeneous catalysis is the difficult separation from the reaction solution. Especially for expensive catalyst or for catalyst which would influence the product properties negatively, the separation is important.

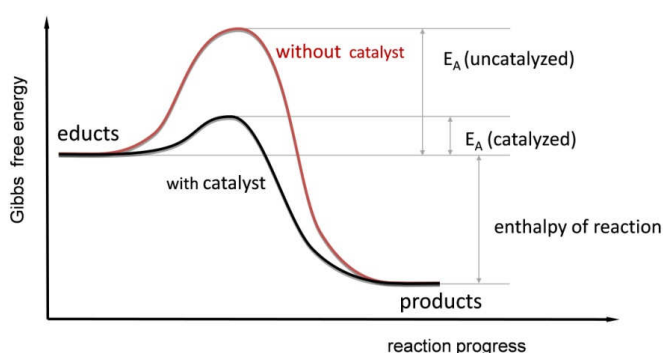


Figure 2-23: Energy diagram of catalyzed and uncatalyzed reaction <sup>[69]</sup>

### 2.6.2. Heterogeneous Catalysis

In heterogeneous catalysis the catalyst and the substrates are in different phases. In technical processes the catalyst is normally in solid state and the substrates are gaseous or liquid, but they contact at the interface. The heterogeneous catalysis can be divided into solid heterogeneous catalysts and immobilized homogenous catalysts.

Mechanisms heterogeneous catalysis: <sup>[70]</sup>

- 1) External diffusion (film diffusion)
- 2) Internal diffusion (pore diffusion)
- 3) Adsorption
- 4) Surface reaction
- 5) Desorption
- 6) Internal diffusion (pore diffusion)
- 7) External diffusion (film diffusion)

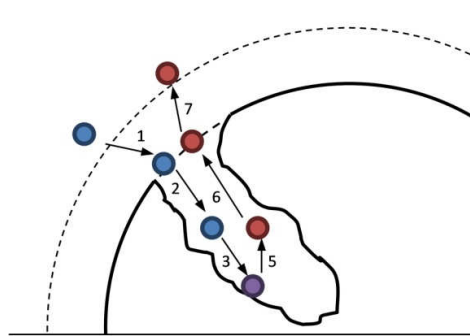


Figure 2-24: Transport processes in heterogeneous catalysis <sup>[70]</sup>

Four of the seven steps concern with the diffusion and hence the diffusion influences the kinetics. In the case of immobilized catalysts on silicon wafers, step 2 and 6 are omitted.

The surface reaction can be further divided into two different mechanisms, the Langmuir-Hinshelwood mechanism (Figure 2-25) and the Eley-Rideal mechanism (Figure 2-26). The two mechanisms are characterized by their adsorption kinetics. In the Langmuir-Hinshelwood mechanism both educts are adsorbed on the surface, therefore the reaction rate is dependent on the surface coverage of both molecules. In addition, the surface coverage is also dependent on the partial pressure of both educts. The reaction rate in the Eley-Rideal mechanism only depends on the coverage of educt A. At a constant partial pressure of educt B, the reaction rate is only a function of the partial pressure of educt A. <sup>[68]</sup>

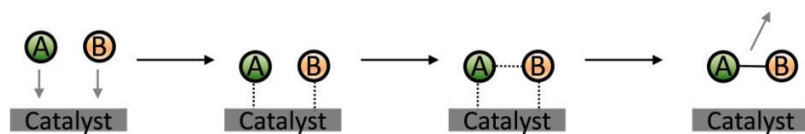


Figure 2-25: Langmuir-Hinshelwood mechanism <sup>[68]</sup>

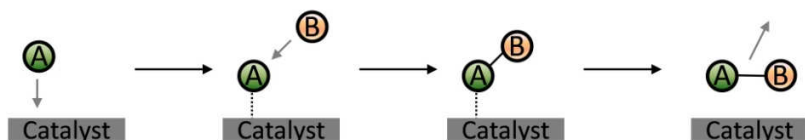


Figure 2-26: Eley-Rideal mechanism <sup>[68]</sup>

### **2.6.3. Phase-transfer Catalysis**

The phase-transfer catalysis is able to accelerate the reactions of two reactants in two different immiscible liquid phases. Therefore the catalyst enables the migration of one reactant into the other phase where the reaction takes place.

### **2.6.4. Biocatalysis**

Biocatalysis is the acceleration of the reaction rate through enzymes or less frequently through ribozymes.<sup>[103]</sup>

Enzymes are proteins with catalytic activity. Beyond the amino acid chains, enzymes can also contain metal centers and sites for co-enzymes/co-substrates. Biocatalysts can act either as homogeneous as well as heterogeneous catalysts.

The key benefits of enzymes are special qualities in chemo-selectivity, regioselectivity and enantioselectivity. Generally, the reaction conditions have to be milder than in the case of the classical enzymes. Most enzymes have their maximum activity at physiological conditions, temperatures between 30 and 40°C and moderate pH values.

In biocatalysis three processes can be distinguished, the process with isolated enzymes, the process with living cells or with dead cells. The decision, if the process is driven with cells or with isolated enzymes, depends on the catalytic step. When three or more enzymes and co-factors are involved in the reaction, the process should be carried out with living cells. The continuous addition of co-factors would increase the process costs enormously. Living cells have efficient systems for co-factor regeneration.

For reactions with 3 enzymes but without co-substrates processes can be carried out with dead cells.

For reactions with less than 3 enzymes the proper way is to work with isolated enzymes. The advantage of isolated enzymes is that higher space-time yields can be obtained and the increased stability. The increased stability allows immobilization and therefore continuous processes can be made.

Enzyme classification: <sup>[71]</sup>

EC 1	Oxidoreductases	EC 4	Lyases
EC 2	Transferases	EC 5	Isomerases
EC 3	Hydrolases	EC 6	Ligases

### 2.6.5. Kinetics and Activity

In general the rate of a catalytic reaction is the product of a rate coefficient and a concentration dependent term.

$$\text{rate} = k * f(c_i) \quad (12)$$

The rate coefficient of the overall catalytic reaction is composed of the rate coefficients of the single reaction steps in the catalytic reaction. In many reactions one step is clearly slower than all other steps. This step is denoted as the rate-determining step. The rate-determining step can be the mass transfer step (external, internal diffusion), the adsorption or the chemical reaction step. The rate determining step has to be measured for every catalytic process. The rate coefficient changes with the prevailing conditions. The rate of the chemical reaction is more sensitive to the change in temperature than the mass transfer.

To describe the activity of a catalytic reaction in an easy way the turnover frequency can be used as described in equation (13).

$$\text{Turnover frequency (TOF)} = \frac{\text{number of molecules of a given product}}{\text{numbers of active sites} \times \text{time}} = \frac{1}{A} \frac{dn}{dt} \quad (13)$$

In homogeneous catalysis the number of active sites is linked with the molar amount of catalyst used in the process. In heterogeneous catalysis or biocatalysis the number of active sites can be undetermined [?] and therefore replaced by the area A of the exposed catalyst or by the amount of enzyme used.

In biocatalytic processes the turnover frequency is denoted by  $k_{\text{cat}}$  and can be expressed by the quotient of  $V_{\text{max}}$  from the Michaelis-Menten kinetics and the enzyme concentration  $[E]$ .<sup>[72]</sup>

$$k_{\text{cat}} = \frac{V_{\text{max}}}{[E]} \quad (14)$$

The equation (15) describes the Michaelis-Menten kinetics for a single substrate reaction.  $[S]$  is the substrate concentration;  $K_M$  is the Michaelis constant and describes the substrate concentration where the reaction rate is the half of the maximal reaction rate  $V_{\text{max}}$ .  $V_{\text{max}}$  is the reaction rate at substrate saturation.

Enzyme kinetics features two limiting cases. In the case of a low Michaelis constant and a high substrate concentration the resulting reaction rate is zero order ( $K_M \ll [S]$ , 0.order). If the substrate concentration is low and the Michaelis constant is high, the reaction rate is first order, with the reaction rate  $v = V_{\text{max}}/K_M \cdot [S]$ .

$$\text{reaction rate } v = \frac{V_{\text{max}} \cdot [S]}{K_M + [S]} \quad (15)$$

$K_M$  and  $V_{\text{max}}$  have to be measured for defined media properties (pH, temperature, ionic strength). The ratio  $k_{\text{cat}}/K_M$  is called catalytic efficiency. By comparing the catalytic efficiency for different substrates, information about the substrate specificity is provided. The maximal catalytic activity is given at values between  $10^8$  and  $10^9$ , which corresponds to the value for substrate transport in aqueous solution. At this value the enzyme reaches the catalytic optimum.

The turnover frequency is only valid for fixed pH values, temperature and ionic strength. When these values are changed, the turnover number changes too. The turnover number is measured in a substrate saturation state.

Enzyme	Substrat	$k_{\text{cat}}$	$K_M$	$k_{\text{cat}}/K_M$
Adenosintriphosphatase	Adenosintriphosphat (ATP)	104	0.012	$8.3 \cdot 10^6$
Trypsin	Benzoyl-Arginin	19	0.02	$1.0 \cdot 10^6$
Urease	Urea	20000	4	$5.0 \cdot 10^6$

**Table 2-1: Examples for enzymes and their catalytic efficiency**<sup>[103]</sup>

### **3. Process, Results & Discussion**

The goal of this thesis is to immobilize a model enzyme on spatially defined areas on a silicon wafer with high surface coverage and high catalytic activity. This was realized through covalent attachment of a linker to a clean hydrogen-terminated wafer through UV-lithography and immobilization of the enzyme by activated ester or by epoxide linker-functionalities.

The general process for the functionalization of silicon wafers with biocatalysts includes the following steps:

- ❖ Cutting of silicon wafers
- ❖ Cleaning
- ❖ Etching
- ❖ Immobilization of the linker
- ❖ Activation of the linker\*
- ❖ Immobilization of the biocatalyst

\* dependent on the used linker

#### **3.1. Cutting**

The silicon wafer was cut into quadratic pieces with a side length of 1.7 cm, by scratching the surface with a needle and breaking at the scratched lines. The size of the wafer pieces was given by the dimensions of the photolithographic box (Figure 3-3) and by the dimensions of the test tubes used for the activity tests (Figure 3-8).

Through scratching some small silicon particles splintered. For removing these particles the wafer pieces were rinsed with acetone followed by a rinse with ultrapure water, before entering the cleaning step.

In the thesis the quadratic silicon wafer fragments are simply called wafer.

Calculation of theoretical step with:

The homogeneity of the silicon surface is dependent on the quality of the step flow process and the number of step width. The higher the numbers of steps, the higher the possibility of perfectly flat terraces without etch pits. The disadvantage is that every step is a potential site for inhomogeneity in the attached SAM.

$$L_{terr} = \frac{d_{DL}}{\tan(\alpha^{\circ})} \quad (16)$$

The theoretical step width on terraces  $L_{terr}$  is given through the equation (16). The height of a silicon double layer  $d_{DL}$  (figure 1-1) is divided through the tangent of the off orientation angle  $\alpha^{\circ}$ .<sup>[73]</sup>

The off-orientation angle of the used wafer is relatively high, which leads to a large number of steps, with narrow step widths. Calculation according to equation (16) leads to a theoretical step width  $L_{terr}(4^{\circ}) = 4,48 \text{ nm}$ .<sup>[74]</sup>

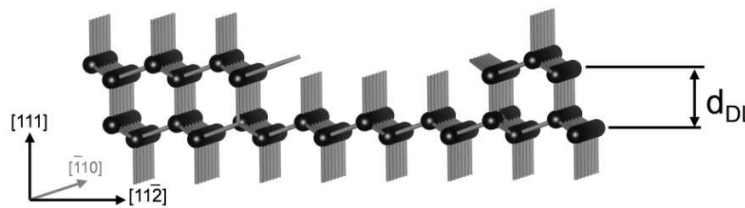


Figure 3-1: Silicon (111) crystal with silicon double layer<sup>[25]</sup>

### 3.2. Cleaning

New wafers are cleaned for 15 minutes in “Standard Cleaning 1” solution and 15 minutes in “Standard Cleaning 2” solution at 80 °C. Used wafers were cleaned in *Piranha* solution at 100 °C for 30 minutes and afterwards with *SC2* at 80 °C for 15 minutes.<sup>[75][76]</sup>

Between and after every cleaning step, the wafers were rinsed copiously with ultrapure water. All cleaning and etching steps were carried out in a PTFE reaction vessel due to the corrosivity of the used chemicals. To avoid contamination of the wafer, the reaction vessel was cleaned for 10 minutes in *SC1* solution.

<i>SC1</i>	5 : 1 : 1	water : H <sub>2</sub> O <sub>2</sub> 30 % : ammonium hydroxide 33 %
<i>SC2</i>	5 : 1 : 1	water : H <sub>2</sub> O <sub>2</sub> 30 % : hydrochloric acid 37 %
<i>Piranha</i>	3:1	H <sub>2</sub> SO <sub>4</sub> 96 % : H <sub>2</sub> O <sub>2</sub> 30 %

### 3.3. Etching

The etching was carried out in two steps. The first step includes a pre-etching step for 30 seconds in HF/Water 1:1 to remove the passivating oxide layer isotropically. The main etching step was carried out in 40 % NH<sub>4</sub>F for 15 minutes<sup>[52]</sup> with 1 % NH<sub>4</sub>SO<sub>3</sub> for deoxygenation.<sup>[52][48]</sup> The reason for the choice of a chemical de-oxygenator was the toxicity and the corrosivity of concentrated fluoride solutions. By sparging with argon gas the risk of aerosol building and accidental spillage is higher and therefore the choice was made on safety issues.

After the etching procedure the wafers were shortly rinsed with ultrapure water and dried in a pure nitrogen gas stream.

For the immobilization steps the wafers were transferred to a glove box, to avoid extensive contact with atmospheric oxygen.

### 3.4. Immobilization of Linker Molecule

#### A) Undecenoic Acid

+ Activation with *N*-Hydroxysuccinimide (NHS) /

1-Ethyl-3-(3-dimethylaminopropyl)carbodiimid (EDC)

#### B) Epoxyhexene/Epoxydecene

The linker molecules were immobilized through UV-induced hydrosilylation on H-terminated Si(111) surface in N<sub>2</sub> atmosphere in a glove box.<sup>[81]</sup> A mercury-vapor lamp was used as UV-source with the main emission of 254 nm and the wafer was irradiated for 2-3 h. It depended on further use if the wafer was functionalized on one side or on both sides.

For all FTIR measurement the wafers were functionalized on both sides, to get a double density of functional surface groups for transmission measurements.

Degassing Solutions:

All solutions were made of dry solvents and were additionally degassed. The dry solvent and the immobilization chemical were weighed into a dry Schlenk tube under argon gas flow. Alternatively a 25 mL two-necked flask could be used with 1 neck equipped with a valve.

Degassing steps: <sup>[77]</sup>

1. The Schlenk tube was placed in a Dewar filled with liquid nitrogen, until the whole content of the Schlenk was frozen
2. The valve was connected to the Schlenk line and the Schlenk tube was set under vacuum until the pressure in the tube did not change anymore
3. The valve was closed and the Dewar with liquid nitrogen was replaced by a water bath. During the thawing of the solution the solved gas escaped in bubble form
4. Then steps 1-3 were repeated four times

The degassing step is important to achieve oxide free SAMs on the silicon. Oxygen is more reactive than the alkene linker at UV- induced reaction conditions. Only small amounts of oxygen are sufficient to form undesirable surface oxides.<sup>[56]</sup>

### **3.4.1. Linker with Terminal Activated Ester Group**

The silicon surface was reacted with 10-undecenoic acid (Figure 3-2) through UV-induced hydrosilylation for 3 h. For this purpose the wafer was immersed in the degassed solution and covered with a fused silica window. The fused silica window was used to prevent the fast evaporation of the solvent. After the irradiation period the wafer was transferred out of the glove box and rinsed with cyclohexane. To remove physisorbed molecules the wafer was cleaned in the ultrasonic bath in cyclohexane and then rinsed copiously with dichloromethane.



**Figure 3-2: Functionalization of Si(111)-H surface with undecenoic acid (UA)**

The UV-hydrosilylation reaction itself is a well-established reaction way, so the attention was turned to the characteristics of the reaction solution. The critical point in the reaction is the layer thickness and the concentration of the wetting solution. Both parameters influence the transmission of the UV-light. Therefore these two parameters were varied.

To show the results of the immobilization variants, the fused silica window in the hydrosilylation step was changed against a photolithographic mask. The quality of the produced pattern was checked by a breath test. The procedure of the test is to breathe respiratory air onto a cooled silicon surface, which causes condensation of the humidity of the respiratory air. Due to the differences of hydrophilicity, size, amount and shape of the condensed water droplets differ on the un-irradiated to the irradiated spots on the wafer. In a former work by *LICHTENEGGER* <sup>[78]</sup>, good results could be obtained for organometallic linker groups with good light contrast.

In the case of an undecenoic acid linker (or epoxydecene linker) the contrast is much lower, but still patterns for visual examination could be observed. Through the low contrast the examination with a light microscope is only possible for the largest patterns.

Variation of concentrations:

10 % undecenoic acid in toluene <sup>[75]</sup>

10 % undecenoic acid in cyclohexane

10 mM undecenoic acid in cyclohexane

Variation of solution layer thickness:

- ❖ Layer thickness 50  $\mu\text{m}$  through “Lichtenegger-adjustment” in lithographic box (1 piece of wafer as distance plate)
- ❖ Layer thickness 200  $\mu\text{m}$  in lithographic box with 2 microscope glass slides as distance plates
- ❖ Layer thickness 350  $\mu\text{m}$  in lithographic box with 1 microscope glass slide as distance plate
- ❖ Layer thickness 500  $\mu\text{m}$  in lithographic box without distance plates

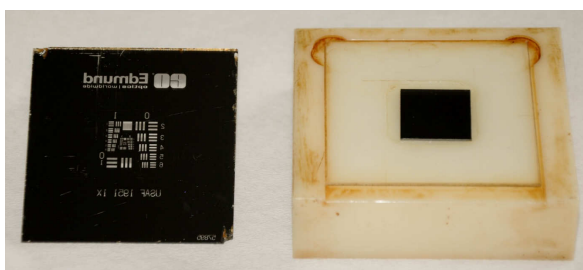


**Figure 3-3: Lithographic box covered with fused silica window; photo mask (left)**

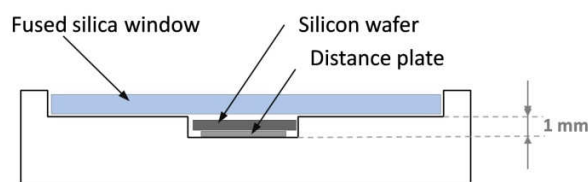


**Figure 3-4: Side view lithographic box**

The use of the reaction solution (10 % undecenoic acid in toluene) reported by VOICU et al. didn't show any results. They carried out the reaction in a photochemical reactor with high UV intensity (12 x 75 W). As toluene is absorbing UV light in the range of the emission spectrum of the UV source <sup>[79]</sup>, the solvent was replaced by cyclohexane.

The solution with the high concentration of 10 % showed only very weak or no patterning with all different layer thicknesses.

Better results were obtained when the concentration was lowered to 10 mmol/L. <sup>[81][80]</sup>

Other papers reported the use of neat alkenes. In the case of undecenoic acid this was not possible as the melting point is slightly above the room temperature, and heating was not possible in the glove box.

The best results were shown in the cases with 200  $\mu\text{m}$  layer thickness (Figure 3-5). The whole pattern of the mask was visible in the breath test, but the contrast is rather low. That only allows the microscopic measurement of the area with the pattern with large line width.

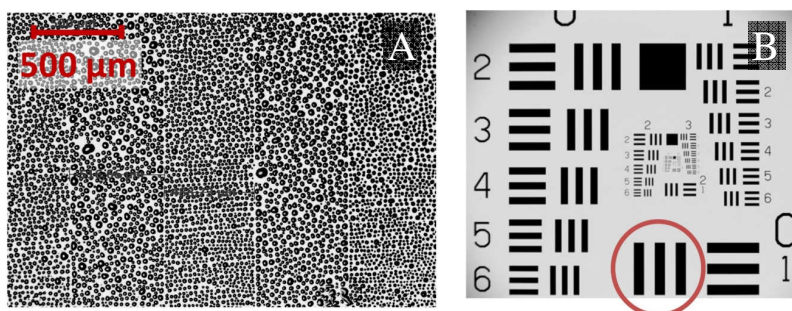


Figure 3-5: Pattern on silicon wafer (A); 1951 USAF resolution test chart (B)

Line-width with functionalization: 516  $\mu\text{m}$

Line-width without functionalization: 488  $\mu\text{m}$

The UV-hydrosilylation leads to a broadening of the line with of 8  $\mu\text{m}$  on each side. One could assume that a part of the broadening stems from the radical chain reaction.<sup>[56]</sup> But even 80 radical reaction steps in a single direction are only accounting for a broadening of 26 nm.

The main part of broadening comes from the distance between the mask and the wafer. As the light from the light source is not perfectly parallel this leads to broadening. The solution could be to use an optical lens between the light source and the photolithographic box.

The patterning lost some contrast during the exposure to atmospheric oxygen, but the pattern was still visible after two weeks.

### 3.4.2. Linker with Terminal Epoxy Group

The silicon surface was reacted with an epoxy functionalized linker through UV-induced hydrosilylation as shown in Figure 3-6. The reaction time was set to 2 hours per side. The first immobilization experiments were carried out with 1,2-epoxy-5-hexene. The immobilization with epoxyhexene showed no patterning. The linker was then changed to 1,2-epoxy-9-decene, as described by *JEANQUARTIER* et al.<sup>[81]</sup> The length of the chain should have a positive influence on the homogeneous arrangement of the SAM and better passivation characteristics.

After the irradiation the wafer could be transferred out of the glove box. To remove the solution and the adsorbed molecules the wafer was cleaned in the ultrasonic bath in cyclohexane and then rinsed copiously with cyclohexane. After drying in a nitrogen stream the samples were stored in a plastic test tube.

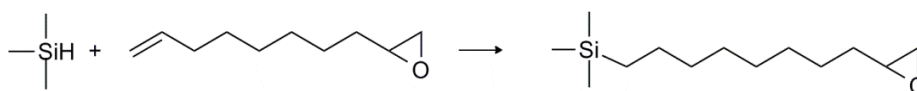


Figure 3-6: Functionalization of Si(111)-H surface with epoxy linker

The solution concentration used was the same as the concentration of carboxylic acid (10 mM) and the wetting layer thickness was varied. Again the best result was obtained at 200  $\mu\text{m}$  but the visible patterning by 1,2-epoxy-9-decene was much weaker as in the case of undecenoic acid.

### 3.5. Activation of Linker Molecule

The epoxide linker is already immobilized in the active form and no additional reaction step is needed prior to enzyme immobilization.

However, the reaction rate between undecylenic acid and the amino group of an enzyme would be too slow.<sup>[82]</sup> Therefore, the carboxylic acid was activated.

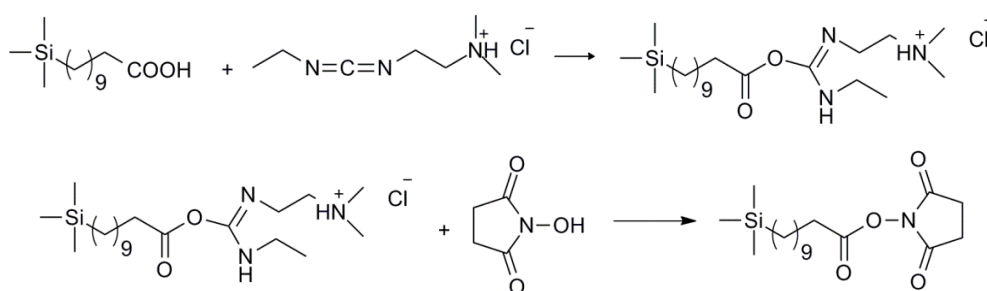


Figure 3-7: Activation of terminal carboxylic acid with NHS/EDC

For the activation of the immobilized wafer the terminal carboxylic acid was reacted with NHS and EDC. The reaction scheme is shown in Figure 3-7. EDC is the coupling reagent between the carboxylic acid and the *N*-hydroxysuccinimide.

The wafer was immersed in a mixture of 5 ml 50 mM aqueous NHS solution and 5 mL 50 mM aqueous EDC solution in a glass tube.

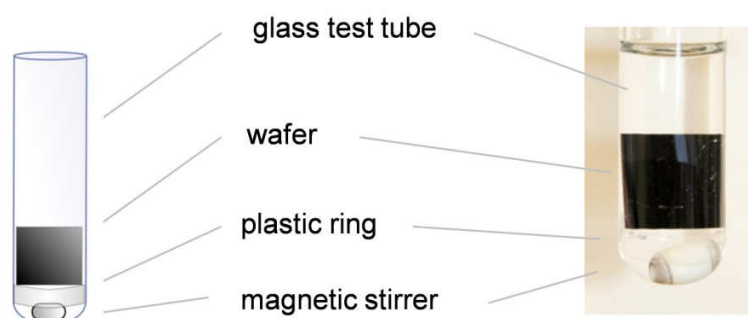


Figure 3-8: Reaction vessel for linker activation, enzyme immobilization and activity tests

The reaction was carried out for 1 h at room temperature and with constant stirring. The reaction arrangement is shown in Figure 3-8. To avoid contact of the stirrer with the wafer a plastic ring was used to create some space between both.

### 3.6. Enzyme Immobilization Step

The enzyme immobilization for the two different linker groups was carried out in the same way. The main difference was the reaction time. The reaction scheme for the activated ester is shown in Figure 3-9 for the epoxide in Figure 3-10.

The enzyme immobilization step was again carried out in a stirred glass tube. The concentration of the enzyme solution was a 1:10 dilution with buffer solution.

The reaction time for the activated ester was 2-3 h, for the epoxide linker 24 - 48 hours. Both reactions were carried out at room temperature.

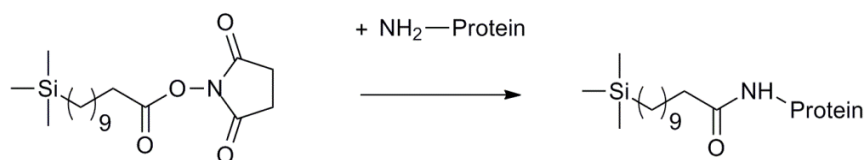


**Figure 3-9: Immobilization of protein on activated ester surface (NHS-UA)**

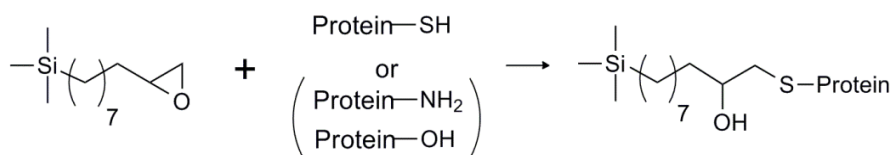


**Figure 3-10: Immobilization of protein on epoxide terminated surface**

### 3.7. Water Contact Angle Measurement

The water contact angle measurement is a method to quantify the wetting angle of a water droplet at the liquid/gas/solid interface on a solid surface. The wetting angle is dependent on the physical properties of the surface, on the hydrophobic /hydrophilic properties, respectively. Functional groups and their homogeneity on the surface affect these properties.

Especially for SAMs, the measurement is an easy but efficient method to evaluate surface substitutions, as the substitution is usually accompanied by a change of hydrophobicity of the surface.

For the measurement a water droplet is placed on the surface and due to the attractive or repulsion forces between the droplet and the surface, a specific droplet form is built. The angle between the surface and the tangent of the droplet at the surface is measured. When the hydrophilicity of the surface is high, then the contact angle is low and the drops are flat.

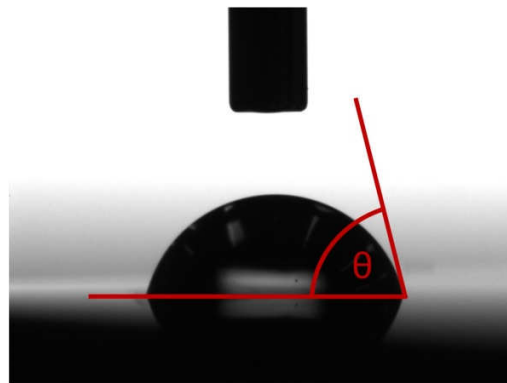


**Figure 3-11: Water contact angle  $\theta$**

For the contact angle measurement a drop of 1  $\mu\text{L}$  deionized water was placed on the wafer. The analysis of the contact angle was done by digital evaluation. An image of the drop was taken and a circle fitting method (H/W method) was used to measure the angle between the surface and the tangent of the droplet.

Every measurement was repeated 6 times on different spots of the wafer.

**Table 3-1 Water contact angle of oxide layer**

	measured values	literature values
Wafer – Natural Oxide	$19.7^\circ \pm 7.7$	$27^\circ$ [83]
After etching and oxidation in $\text{H}_2\text{O}_2$	$\approx 5^\circ$	$<10^\circ$ [84]

The distribution of low contact angles is rather broad because of microscopic scratches. The values of contact angle less than  $10^\circ$  can only be estimated, an exact measurement is not possible anymore.

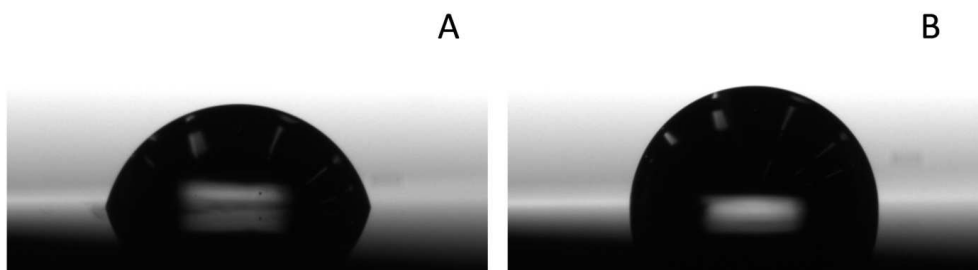


**Figure 3-12: Water contact angles,  $76^\circ$  (A);  $89^\circ$  (B)**

Wafer H-terminated:  $89.8^\circ \pm 0.8$

H-terminated wafers showed good results with narrow distributions. As expected the contact angle changed significantly between the hydrophilic silicon oxide and the hydrophobic H-terminated surface. In literature the contact angle is reported to be around  $80^\circ$ .<sup>[83][85][86]</sup>

This is also visible in the cleaning and etching procedure. After cleaning in *SC1* and *SC2*, as already described before, the surface of the wafer is obviously hydrophilic, with large, flat drops. Already after the short pre-etch in hydrofluoric acid the surface wetting changes drastically. Only a few, small drops are visible which are dripping of easily.

Wafer COOH terminated:  $75.5^\circ \pm 2.1$

Wafer COO - enzyme:  $69.4^\circ \pm 5.0$

The acid-functionalized wafer showed constant measurement values on the fully terminated and on the half-half wafers. The values differ clearly from the H-terminated and the oxidized wafer. In the literature the contact angle for acid terminated surfaces is reported to be around  $10^\circ$  lower at  $65^\circ$ .<sup>[85][87]</sup> This difference should be related to a lower coverage of the surface. The enzyme immobilization shows a broad distribution of contact angles on the surface. In general the values for fully enzyme covered surfaces were expected to be lower, by reason of the water solubility of the protein. The broad distribution of the water contact angle indicates an inhomogeneous immobilization of the enzyme. This is caused on the one hand to the surface density of the enzymes and on the other hand to miscellaneous orientations of the immobilized enzymes.

Wafer epoxide terminated:  $82.5^\circ \pm 2.7$  <sup>[88][89]</sup>

Wafer epoxide enzyme:  $72.9^\circ \pm 3.5$

In the case of the undecenoic acid linker also a half-half wafer was produced. Therefore one half of the wafer was covered by aluminum foil, to prevent functionalization by UV-hydrosilylation.

Wafer 50/50

COOH terminated:	$76.1^{\circ} \pm 2.0$
Non-functionalized:	$81.6^{\circ} \pm 1.7$

Wafer 50/50

Enzyme terminated :	$68.9^{\circ} \pm 5.9$
Non-functionalized:	$67.4^{\circ} \pm 5.6$

At the beginning of the process the non-functionalized parts are H-terminated. During the following process steps, they were exposed to humidity and atmospheric oxygen and were subjected to the natural oxidation processes. The different process ways of the two half-half wafers explains the differences in their water contact angle. The acid terminated wafer was transferred from the glove box to a closed test tube. The enzyme terminated wafer was in contact with different aqueous solutions during the process (activation step, enzyme immobilization, enzyme activity test). All in all, it was surprising that still both values for the non-functionalized parts were very high. This indicates that the Si-H surface is partially stable even for longer periods.

### 3.8. FTIR Measurement

The Fourier transform infrared spectroscopy is a method to detect functional groups through detecting the absorption of mid- infrared light. Functional groups with an electric dipole moment can absorb the electromagnetic radiation in a specific range in the IR spectrum. The IR light is absorbed at specific vibration frequencies of chemical bonds. This gives semi-quantitative information of the presence of functional groups and contaminations of a sample.<sup>[29]</sup>

The IR measurement can be carried out in different modes, like transmission mode or reflection mode. In the transmission mode the IR beam passes through the sample. The FTIR measurement was carried out in the transmission mode. To identify the best transmission setting, the angle of incidence of an H-terminated wafer sample was varied between 20 and 90°. Additionally the aperture value was varied. The best parameters were found to be an angle of 45° of the sample holder and a aperture value of 1.5 cm. During the different experiments FTIR spectra were recorded with these adjustments.

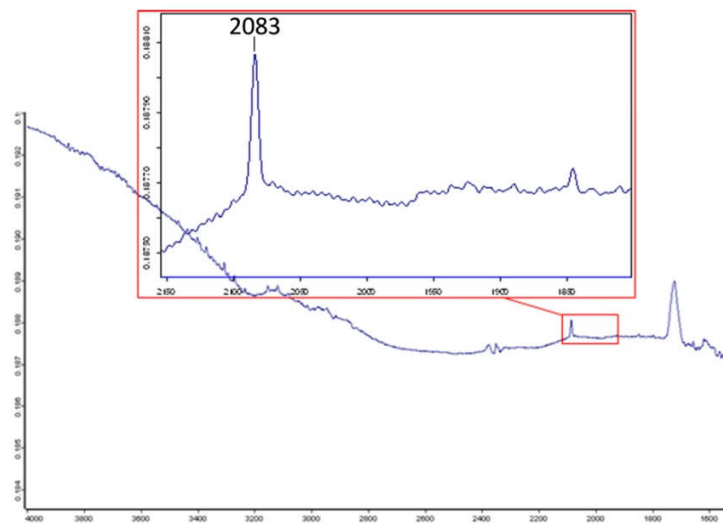
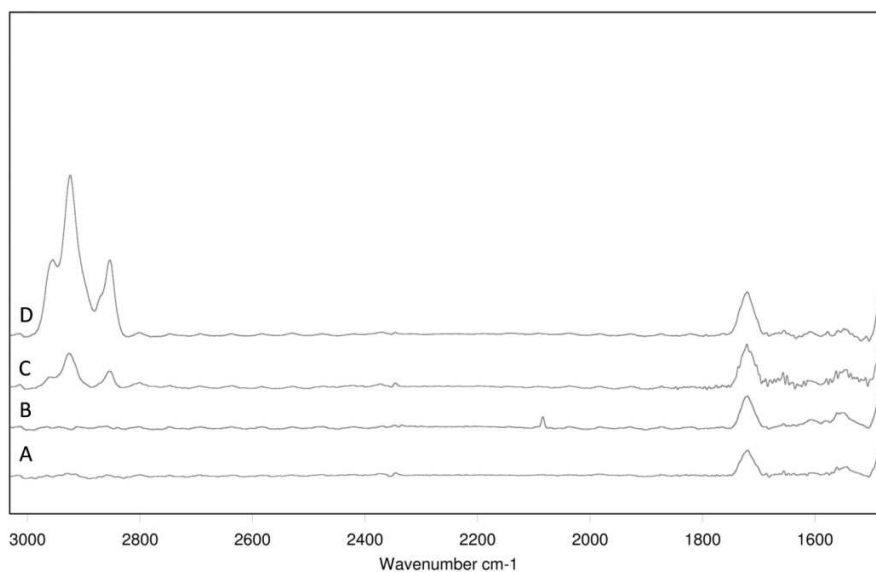


Figure 3-13: FTIR transmission spectrum of a Si(111)-H wafer

The FTIR spectrum of an H-terminated wafer is shown in Figure 3-13. The narrow peak at  $2083\text{ cm}^{-1}$  is related to the Si(111)-H bond. The absence of peaks at  $2259\text{ cm}^{-1}$  and  $2002\text{ cm}^{-1}$ , which are related to  $\text{O}_3\text{SiH}$  and  $\text{O}_2\text{SiH}_2$  indicate the absence of silicon oxides. Furthermore, the missing peaks at  $2115\text{ cm}^{-1}$  and  $2140\text{ cm}^{-1}$  indicate that only Si-H and no  $\text{SiH}_2$  and  $\text{SiH}_3$  are present on the surface.<sup>[35][80]</sup>



**Figure 3-14: FTIR transmission spectrum Si-wafer**  
(A) oxidized wafer, (B) H-terminated, wafer with carboxylic acid linker (C) and with epoxide linker (D)

In Figure 3-14 the FTIR spectra of the bare wafers and the spectra of the immobilized linker groups are shown. The peak at  $2083\text{ cm}^{-1}$  is related to the H-termination of the surface, as described before. This peak is missing in the oxidized wafer. All wafers showed a peak between  $1700\text{ cm}^{-1}$  and  $1750\text{ cm}^{-1}$ . This peak was even present at freshly oxidized (A) and freshly etched samples (B). This peak is not described in literature and is probably related to some surface contamination.<sup>[75][76][90]</sup> The peaks at  $2925\text{ cm}^{-1}$  and  $2855\text{ cm}^{-1}$  are related to the antisymmetric and symmetric  $\text{CH}_2$ -stretching vibrations and are the confirmation that linker groups are immobilized. In the spectrum of the carboxylic acid the  $\text{C}=\text{O}$  stretching is not visible and is probably masked by the peak between  $1700\text{ cm}^{-1}$  and  $1750\text{ cm}^{-1}$ . The absence of the peak at  $1640\text{ cm}^{-1}$ , which is related to the  $\text{C}=\text{C}$  double bond, is evidence that the linker is only bound through a hydrosilylation reaction and not through a reaction of the functional group with the  $\text{Si}-\text{H}$  group.<sup>[75]</sup>

For all samples the FTIR measurements in the transmission mode proved difficult, as the signal to noise ratio is quite small, further the water and the  $\text{CO}_2$  peaks affected the spectra, even with extensive  $\text{N}_2$ -rinsing.

The solution of the water / CO<sub>2</sub> problem could be the measurement in high vacuum. To solve the problem of the low signal the literature describes two advanced ways to measure surface molecules on silicon. Both methods are attenuated total reflection (ATR) methods:

- a) Internal Reflectance ATR: The silicon wafer itself acts as ATR crystal, with the advantage of multiple internal reflections. The disadvantage is that every wafer has to be grinded on the edges in the right angle, to allow the IR beam to enter the crystal. This means higher efforts on sample preparation and measurement techniques.<sup>[75][76][33]</sup>
- b) Single Reflectance ATR  
The surface of the silicon wafer can be measured by ATR, but a crystal with a higher reflectance index is needed (Germanium Crystal). The advantage of the method is the easy method which is usable for every wafer. The disadvantage is, that the signal to noise ratio is not as good as in the Internal Reflectance ATR.<sup>[12][91][92][93][35]</sup>

### 3.9. Enzyme Activity

Laccase (EC 1.10.3.2, p-diphenol:dioxygen oxidoreductase) from *Trametes hirsuta* is a copper containing enzyme and was kindly provided by Prof. Gübitz, Department of Environmental Biotechnology, Graz University of Technology. The enzyme catalyzes the abstraction of a hydrogen atom from aromatic hydroxyl groups of ortho and para-substituted phenolic substrates, followed by the production of a free radical. The radical can further react to a quinone (Figure 3-15) through a second enzymatic conversion or by spontaneous disproportionation.<sup>[94][95]</sup>

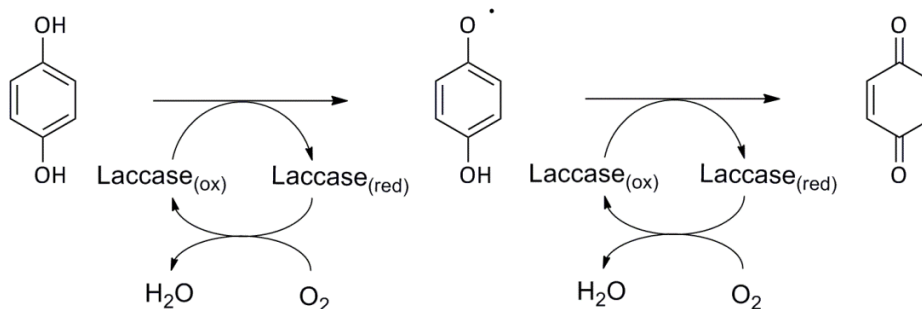


**Figure 3-15: Schematic reaction of the used enzyme with diphenol**

The enzyme was used as a model enzyme because of a high stability and the fact that the enzyme needs no cofactors for catalytic activity.<sup>[96]</sup> The molecular mass of the enzyme is 62kDa<sup>[97]</sup> and has good storage stability at 4 °C at slightly acidic pH.<sup>[101]</sup> Figure 3-16 shows the structure of the enzyme.

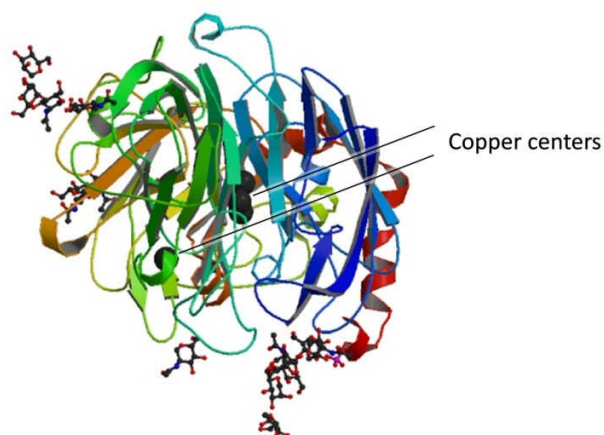


**Figure 3-16: Laccase from *trametes hirsuta***  
Figure from Ref.<sup>[98]</sup>

The oxidation of diphenols is often accompanied by a change of color. This can be used to test the activity of the laccases.

The first activity test was intended to be a simple qualitative visual test. It should show a color change of the solution, if a reaction takes place. As substrate pyrogallol (1,2,3-benzenetriol) was used in high concentrations of about 50 g/L. The disadvantage of pyrogallol is that aqueous solutions are light sensitive. Even in the dark some chemical reaction occurred.

For the activity test a wafer was placed in a test tube and immersed in the substrate solution. Additionally three further test tubes were filled as described in Table 3-2.

**Table 3-2: Visual activity test**

Test Tube	Sample Description	Color reaction
1	Free enzyme + substrate solution	fast, intense
2	Immobilized enzyme + substrate solution	slow, weak *
3	Free enzyme + water	no change in color
4	Substrate solution	slow, weak

\* The weak color reaction seems to stem from the photoreaction and not from enzymatic activity, test tube 2 and 4 showed equal change in color

The proof of the reaction should be given by a difference in color intensity between test tube 2 and the control solution in test tube 4. After 1 hour both tubes clearly changed their color, but color and intensity between the two test tubes were not distinguishable.

To solve this problem the qualitative visual test has been changed to quantitative UV spectroscopy and the substrate has been changed to 2,6-dimethoxyphenol. The new substrate showed better stability against photo reactions. UV-measurement of the substrate solution showed no reaction with light during the measurement period of one hour.

The reaction by the substrate with enzyme solution was again fast and intense, but this time the produced radical showed some degradation reaction, with resulting loss of light absorption. This degradation was slow for low substrate concentrations. As it was not clear if this reaction is photo-induced, all reactions were carried out in the dark.

The conversion of the substrate was measured with UV/Vis spectroscopy at 470 nm.<sup>[94]</sup> The absorption at 470 nm originates from the conversation of DMP to 3,3',5,5'-tetramethoxy-4,4'diphenoquinone.<sup>[99]</sup>

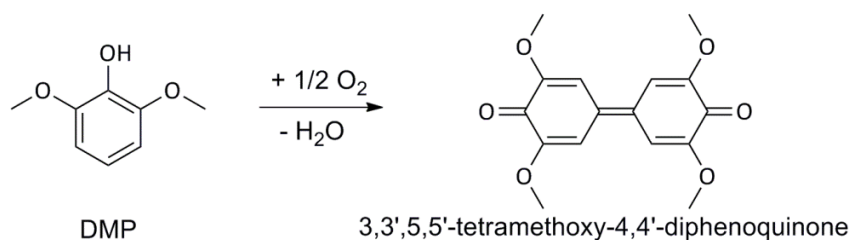


Figure 3-17: Enzymatic conversion of dimethoxyphenol to diphenoquinone <sup>[99]</sup>

### 3.9.1. Optimization of Immobilization pH Value

Enzymes are in general influenced by the pH value of the surrounding media. They are only stable in a certain pH range. Outside of this pH range the enzyme gets destroyed or degenerated in a faster or slower manner, depending on the enzyme. Additionally, the activity of the enzyme is dependent on the pH value of the substrate solution. To ensure maximal reaction velocity, the pH value has to be kept at the optimal reaction pH value.

For immobilization reactions of enzymes there has to be found a compromise. Many chemical coupling reactions also have an optimal pH range. Only in this range good coupling yields can be expected. So on one hand the coupling reaction should give high yields and on the other hand the enzyme should not be distinctly degraded or inactivated during the immobilization step.

The bond formation with the epoxide group has to be either base or acid catalyzed.<sup>[100]</sup> In case of activated carboxylic acid, a higher pH value is preferred to inhibit the hydrolysis with water.

To quantify the relation of the immobilization pH value to the enzymatic activity an enzyme assay was carried out.

The optimal pH value for the activity of the used laccase is reported to be 4.5 <sup>[95]</sup> and for similar laccases 5 <sup>[101]</sup>. To show the activity at optimal pH value compared to a higher pH value some tests were additionally carried out at pH 5.5

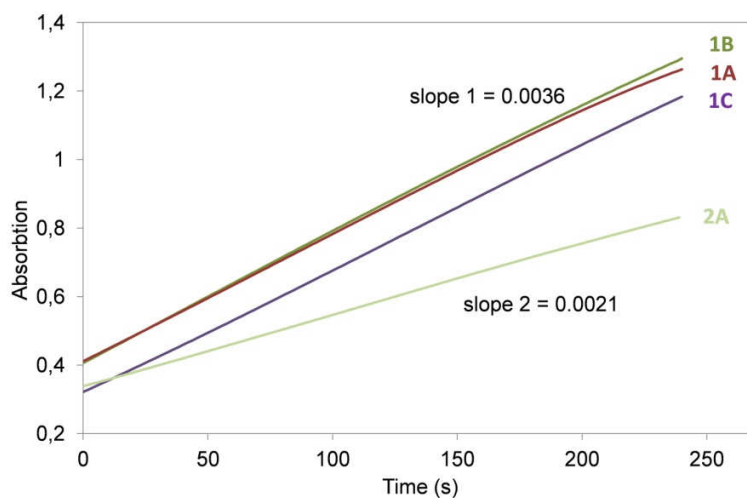


**Figure 3-18: Enzyme assay**  
pH 4.5 at series 1, pH 5.5 at series 2.  
Immobilization pH: 4.5 (1A), 7.2 (1B) and 8.5 (1C)

The enzyme assay should show the short term stability of the enzyme at different pH values. The test was set to two days, as this is the maximal immobilization time for the epoxide linker. For this purpose the enzyme solution was diluted with buffer solution by 1:10. Three samples were made with different buffers. The used buffer solutions were: pH 4.5 Na-citrate buffer (50 mM); pH 7.2 TRIS (2-Amino-2-hydroxymethyl-propane-1,3-diol)/HCl (50 mM); pH 8.5 TRIS/HCl (50 mM). All enzyme solutions were stored at room temperature for two days before measuring the activity. The samples were stirred during the storage time. 15  $\mu$ L of the stored enzyme solution were added to the photometric test solution (1mM DMP, 50 $\mu$ M Na-citrate buffer pH 4.5). The activity of the enzyme solution at pH 4.5 and 8.5 are shown in Figure 3-18 (1A and 1C)

To compare the activity with a fresh enzyme solution, the stock solution was diluted in the same way as the samples (1:10 with buffer pH 7.2). 15  $\mu$ L of this solution was measured at pH 4.5 Figure 3-18 (1B) and at pH 5.5 Figure 3-18 (2A). All enzyme assays were carried out at 25°C.

As expected, the activity test showed that the reaction rate is higher at pH 4.5 compared to pH 5.5. Additionally it could be shown that the stability of the enzyme is given at all immobilization pH values, at least for 2 days, without rendering the activity of the enzyme.

Thus, the immobilization reactions could be carried in the optimal pH range of the coupling reaction.

A calibration standard measurement was made to be able to calculate the activity units of the enzyme solution and the immobilized enzymes. The range of the standards was between 1 and 50  $\mu\text{mol/L}$ . The standard solutions were made of 1.4ml Na-citrate/citric acid buffer (pH 4.5 100mM) of stock solution (100 $\mu\text{M}$  dimethoxyphenol) and filled up with deionized water to a volume of 3 mL. The UV/Vis quartz glass cell was filled with 2.5mL of the standard solutions and 25  $\mu\text{L}$  of the enzyme stock solution were added. After shaking, the absorption was monitored until the absorption reached a maximum value.

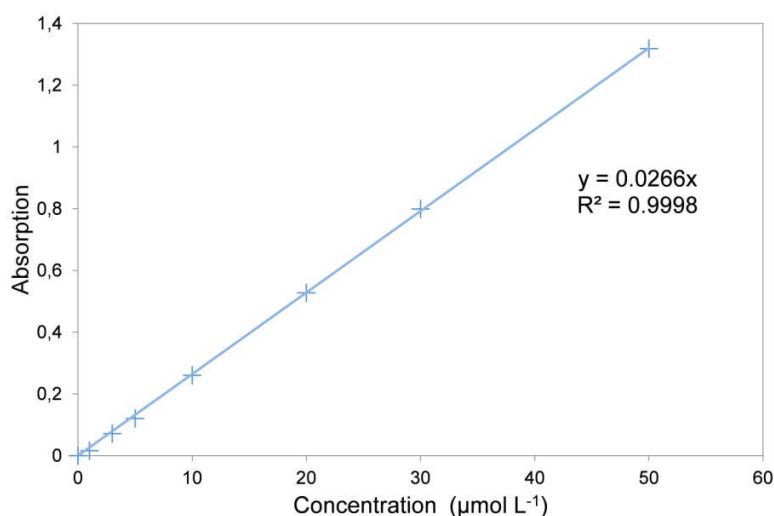


**Figure 3-19: UV/Vis calibration measurement**

Calibration standard slope:	$m_{\text{Cal}} = 0.0266 \text{ abs L } \mu\text{mol}^{-1}$
Slope activity test pH 4.5:	$m_{\text{Act}} = 0.216 \text{ abs min}^{-1}$
Dilution Factor	$f_{\text{D}} = 6 * 10^{-4}$
Enzyme concentration	$c_{\text{Enz}} = 1.0 * 10^3 \text{ mg L}^{-1}$

$$\text{Enzyme activity } U = \frac{m_{\text{Act}}}{m_{\text{Cal}} * f * c_{\text{Enz}}} \quad (17)$$

The activity unit U was defined as the amount of enzyme that converts 1 μmol of DMP per minute. The turnover frequency is the relation of mol DMP converted per second by 1 mol of enzyme.

Enzyme activity	13.5 U / mg enzyme
Molar enzyme activity	8.4 * 10 <sup>8</sup> U / mol enzyme
Turnover frequency (k <sub>CAT</sub> )	14.0 s <sup>-1</sup>

### 3.9.2. Calculation of Maximum Immobilization

The maximum value of immobilized enzyme is calculated for a wafer with 4° miscut angle and assumed that only the hydrogen atoms in (111) direction are functionalized. The maximal substitution of surface hydrogen atoms by linker groups is proposed to be at 50%.<sup>[53]</sup>

Perpendicular Si(111)-H	7.6 * 10 <sup>14</sup>	H atoms / cm <sup>2</sup>	[51]
	1.26	nmol H / cm <sup>2</sup>	
SAMs	3.8 * 10 <sup>14</sup>	linker molecules / cm <sup>2</sup>	
	0.63	nmol / cm <sup>2</sup>	

The laccase (*trametes hirsute*) is in an ellipsoid shape with dimensions of 6.4 x 5.4 x 5.4 nm<sup>[102]</sup> and a molecular weight of 62 kDa. For the calculation of the maximal coverage, the enzymes were taken as spheres with 6 nm in hexagonal alignment on the surface.

This maximal coverage was used to calculate a maximal enzymatic activity of the surface. This maximal enzymatic activity is a hypothetical value which should allow some comparison to the produced wafers.

In practice the hypothetical value will not be reachable, as for the maximal coverage, the enzymes would have to align perfectly and very dense.

This surface density is leading to a loss of activity of the single enzymes.

Maximal enzyme coverage	$3.21 \cdot 10^{12}$	enzymes / cm <sup>2</sup>	[103]
Maximal surface activity	$4.47 \cdot 10^{-3}$	U / cm <sup>2</sup>	

The surface area that is occupied by one enzyme molecule corresponds to approximately 100 underlying linker groups. This value is calculated from the maximal enzyme coverage divided by the maximal linker density. That means, even at lower linker coverage a multipoint immobilization of the enzyme is probable. If the high density of the linker groups is lowering the enzyme activity through multipoint attachment should be explored in further experiments.

### 3.9.3. Activity Measurement Without Stirring

The first activity tests were carried out as in situ measurements as described by *JEANQUARTIER* et al.<sup>[81]</sup> Two wafer pieces were directly placed in a UV/Vis measurement cell parallel to the UV/Vis beam, without disturbing the beam (Figure 3-20, right). To avoid damages of the quartz glass UV/Vis cells by scratching with the wafer, disposal plastic 10mm cells were used. The wafers were immersed in 2.5 mL of 0.5 mM DMP solution at pH 4.5.

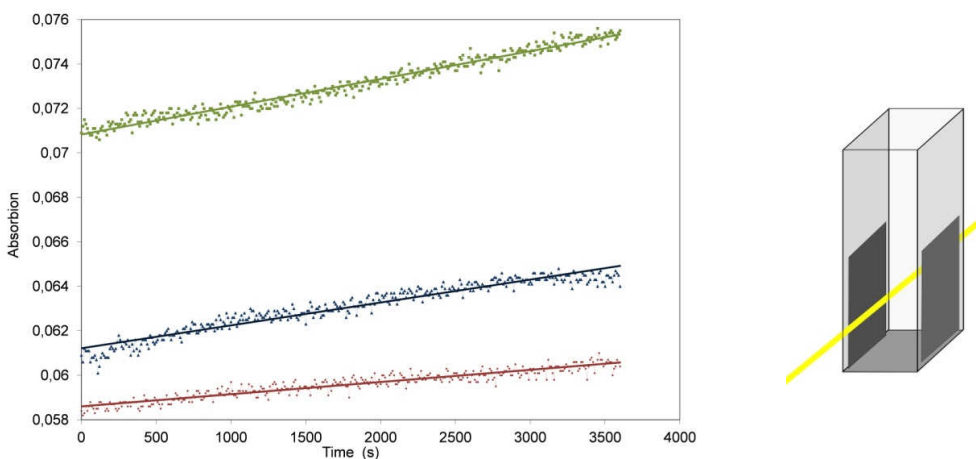


Figure 3-20: Activity measurement without stirring and measurement arrangement

The activity test showed low yields (Figure 3-20) and the spectroscopic measurement showed already a quite high signal to noise ratio.

**Table 3-3: Enzymatic activity of enzyme-UA-wafer without stirring**

Wafer-UA-NHS:			
Immobilization pH	Activity U cm <sup>-2</sup>	relative coverage	relative activity
4.5	1.4 * 10 <sup>-6</sup>	0.033 %	0.033 %
7.2	3.4 * 10 <sup>-6</sup>	0.075 %	0.075 %
8.5	2.8 * 10 <sup>-6</sup>	0.062 %	0.062 %

There are two values that can be calculated for the quality of immobilization, the relative coverage and the relative activity. The values of both percentages are equal and the immobilization quality can either be expressed by the relative coverage or by the relative activity, as shown in Table 3-3.

The relative coverage and the relative activity are the ratios between the present values to the hypothetical values. The relative coverage means that this percentage of the surface is occupied by fully active enzymes. This value can also be expressed in the value of relative activity. The relative activity means that the whole surface is completely covered by enzymes but their activity is at the given percentage.

In reality we will have a higher coverage with not totally active enzymes or in other words, we will have a higher surface activity with only partial covered surface.

The test showed as expected that the immobilization for the activated carboxylic linker is lower at lower pH values. This result was also achieved in further experiments. The values at neutral to slightly basic pH values are in the same range. Therefore the further immobilization reactions were preferentially carried out at neutral pH. The reason is that the laccase is only standing for a model enzyme. Many other enzymes are only stable at neutral pH and therefore a mild immobilization is favored.

The low turnover of the silicon wafer is not only due to the enzymatic activity of the immobilized enzymes but also to transport issues. This could be shown by shaking the UV measurement cell outside of the spectrometer. The tags (\*) in Figure 3-21 are marking the moments when the wafer was shaken. The shaking is accompanied by an increase of absorption. The further experiments were carried out ex-situ accompanied by stirring, in the reaction arrangement described in Figure 3-8.

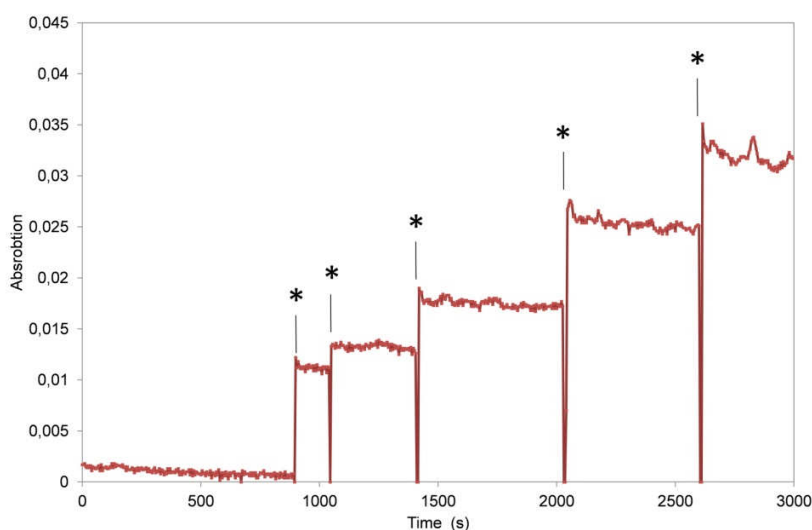


**Figure 3-21: Enzymatic activity measurement with shaking, \* point of shaking**

#### 3.9.4. Ex-situ Activity Measurements

The wafers were immersed in 10 ml 0.5 mM substrate solution in buffer with a pH value of 4.5. The reaction glass tube was additionally covered with aluminum foil to prevent photochemical reactions. Every 5 minutes a sample of 2.5 mL was taken and measured with UV/Vis spectroscopy. The sample was poured back into the reaction tube immediately after measuring. The measurement duration was set between 30 and 60 minutes.

Measurement of an epoxide-wafer with enzyme immobilization at pH 8.5 (one day stored in buffer solution) showed an activity of  $2.7 \cdot 10^{-6} \text{ U/cm}^2$  (0.53 % relative activity) which was about one order of magnitude higher than in the tests without stirring, as described in 3.9.3. The ex-situ activity measurement showed to elevate the transport of the substrate to the enzyme. The stability test in section 3.9.5. was

carried out as an ex-situ activity measurement. In this section the immobilization was showed for an epoxide wafer at pH 4.5 and an activated ester wafer at pH 8.5.

### 3.9.5. Stability Test

The activity of epoxide and carboxylic acid wafers was measured (as described in 3.9.4. ) directly after immobilization of the enzyme. The wafers were only rinsed with water before transferring to the substrate solution. After the first activation measurement run the wafers were washed again with deionized water and a second run was started. After the second run the wafers were stored in a buffer solution at pH 4.5 at 8°C. After 1 day, 3 days and 7 days the activity assay was repeated.

Both wafer series showed a distinct difference in activity between first and second run. This effect can be most likely be related to a loss of adsorbed enzymes and not to a loss of activity of the immobilized enzymes. This is based on the assumption that if the immobilization would lead to a loss of activity, this would happen immediately, not after the first two runs. Additionally, the loss of activity through degradation is improbable at the storage conditions (pH 4.5, 4°C), as this is also not observed for the stem enzyme solution. This awareness is also valid for the decrease between the second and the third run. The activity after the two fist runs kept then staying constant.

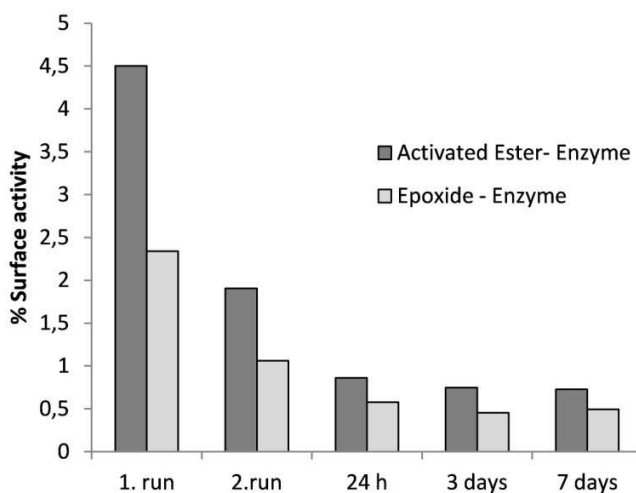


Figure 3-22: Stability Test

**Table 3-4: Stability test; wafer with activated ester linker**

Wafer-UA-NHS:			
activity test	activity U cm <sup>-2</sup>	relative activity	coefficient of determination
1. Run	2.0 * 10 <sup>-4</sup>	4.50 %	0.99
2. Run	8.5 * 10 <sup>-5</sup>	1.90 %	0.95
24 h	3.9 * 10 <sup>-5</sup>	0.86 %	0.97
3 days	3.3 * 10 <sup>-5</sup>	0.74 %	0.87
7 days	3.3 * 10 <sup>-5</sup>	0.73 %	0.87

The actual activity of the wafers was proposed to be at the value after 24h.

**Table 3-5: Stability test; wafer with epoxide linker**

Wafer-Epoxyde:			
activity test	activity U cm <sup>-2</sup>	relative activity	coefficient of determination
1. Run	1.0 * 10 <sup>-4</sup>	2.33 %	0.99
2. Run	4.7 * 10 <sup>-5</sup>	1.06 %	0.99
24 h	2.6 * 10 <sup>-5</sup>	0.58 %	0.89
3 days	2.0 * 10 <sup>-5</sup>	0.46 %	0.97
7 days	2.2 * 10 <sup>-5</sup>	0.49 %	0.87

The value of the epoxide wafer with enzyme immobilization at pH 8.5 from 3.9.4. was compared with the activity from the stability test after 24h. Both wafers showed approximately the same activity at around 0.5% relative activity. This proved that the immobilization by epoxy groups can either carried out acid or basic catalyzed.

### 3.10. X-ray Photoelectron Spectroscopy (XPS)

X-ray photoelectron spectroscopy is a way to analyze the elemental composition of a surface. The basic principle is to irradiate a sample with electromagnetic radiation which sufficient energy to eject core electrons as photoelectrons. The binding energy of electrons is dependent on the element. The photoelectrons are detected and can be assigned to certain elements. The measurement depth is between 5 and 10nm and beside hydrogen and helium all elements can be detected.<sup>[104]</sup>

The samples were measured by Assoz. Univ.-Prof. Dr. Georg Koller from the Institute for experimental Physics (Surface Science Group) at the Karl-Franzens University. The wafers were kept in vacuum for 12h before measurement ( $10^{-8}$  mbar). The results of the measurement are shown in Table 3-6.

**Table 3-6: Results X-ray photoelectron spectroscopy measurement**

	Si	O	C	N
Epoxide	29 %	22 %	49 %	0 %
COOH	36 %	20 %	44 %	0 %
COOH-enzyme	29 %	31 %	38%	2 %

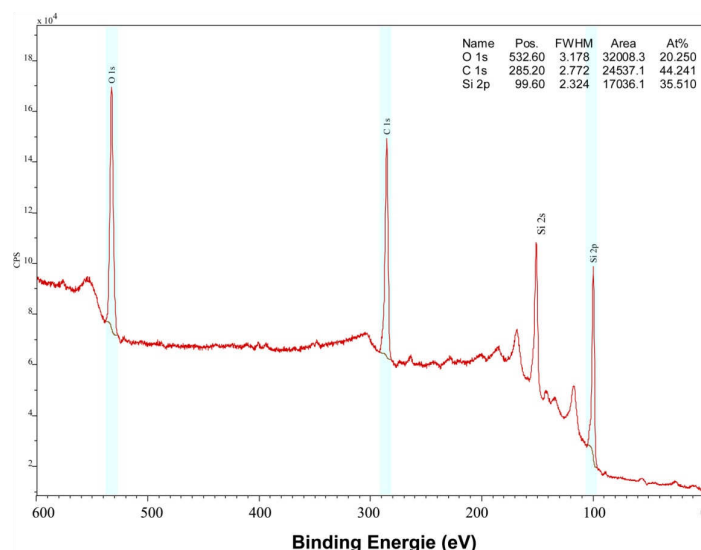


**Figure 3-23: XPS spectrum of wafer with immobilized undecenoic acid linker**

The wafer with immobilized UA linker showed only silicon, oxygen and carbon peaks, which was in consistence with the expectations. The theoretical proportion of oxygen to carbon is 2:11 (= 0.182) for undecenoic acid, as shown in Table 3-7. All values in Table 3-7 are calculated out of the molecular formula, the elemental composition for the laccase is calculated out of the amino acid composition and the ligands.<sup>[97][105]</sup> The measured value for the oxygen to carbon value is 1:2.2 (= 0.455) which is more than double as high as the theoretical value. This should be related to silicon dioxide, which is confirmed by a visible shoulder of the Si peak, in the narrow scan. The silicon dioxide is formed after the immobilization of the linker through interaction of atmospheric oxygen and humidity. The fact that silicon oxide formation was enabled, speaks for a insufficient functionalization by the linker groups. Only with adequate space between the alkane chains, surface oxidation is possible.

**Table 3-7: Elemental compositions of linkers and enzyme**

	C	N	O	S	P	Cu
Epoxydecene	10	-	1	-	-	-
Undecenoic acid	11	-	2	-	-	-
Laccase	2795	678	884	9	1	4

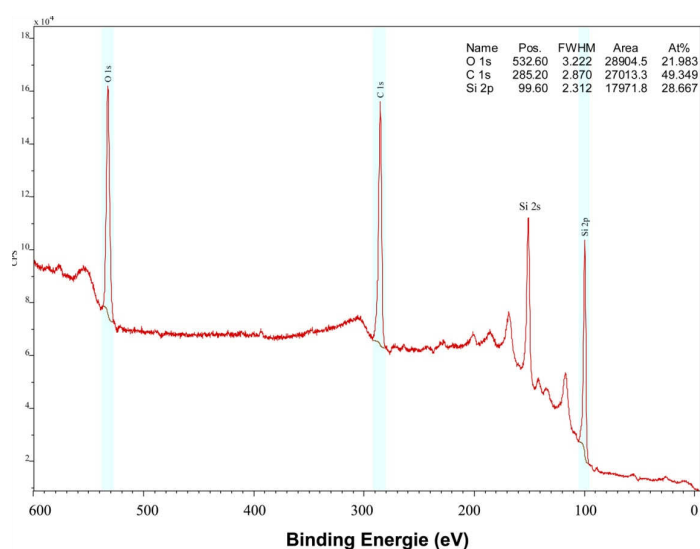


**Figure 3-24: XPS spectrum of wafer with immobilized epoxid linker**

The wafer with immobilized epoxydecene (ED) showed similar results as the undecylenic acid-wafers in Figure 3-24. Only silicon, oxygen and carbon atoms are visible. For the epoxide wafer the difference between expected and observed C:O value is even higher. The expected value is 1:10 (= 0.10) and the observed value is 1:2.25 (=0.44).

The spectrum for the immobilized enzyme was measured with an activated ester-wafer. The surface showed nitrogen peaks, which indicates a immobilization of a considerable amount of enzyme. The proportion between carbon to nitrogen was expected to be higher. One reason could be the insufficient immobilization of the surface by the enzyme. The second reason could be the accompanying immobilization of other organic compounds with lower nitrogen content. These compounds can stem from the crude enzyme stem solution. The possibility that the nitrogen is stemming from unreacted NHS groups is implausible. The wafer was stored in aqueous buffer solution at pH 4.5. At these conditions the activated ester hydrolyzes.<sup>[106]</sup>

The absence of the signals related to sulfur phosphorus and copper are related to their low content under 0.1%.

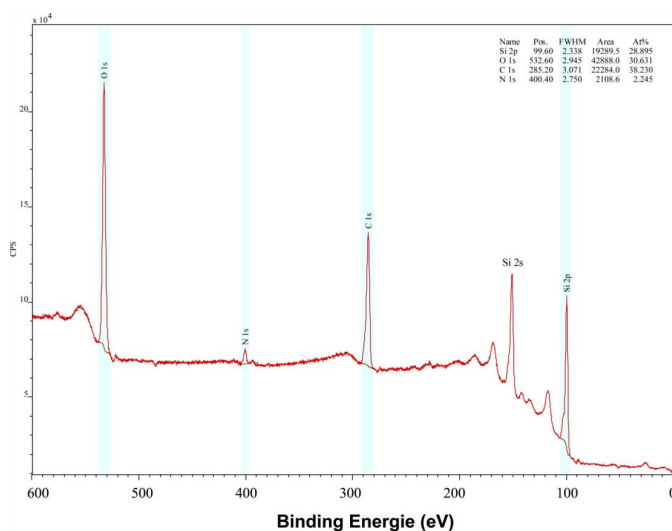


Figure 3-25: XPS spectrum of wafer with immobilized enzyme via NHS-UA-linker

#### 4. Summary & Outlook

The model enzyme laccase from *trametes hirsuta* was immobilized on flat Si(111) wafer surfaces using two different linker molecules.

All silicon wafers were etched in a two-step process by hydrofluoric acid followed by deoxygenated 40% ammonium fluoride solution and characterized by FTIR and water contact angle measurements.

The linker systems were 1,2-epoxy-9-decene and 10-undecenoic acid. The first reaction step for the linker systems was the attachment to the silicon surface through a UV-induced hydrosilylation. Samples with patterns have been prepared by using a photomask and patterns were visible by optical microscopy. The immobilized epoxydecene could be directly used as linker to the enzyme whereas the acid had to be activated to an ester.

The stability of the enzyme was shown for two days for pH values between 4.5 and 8.5, therefore the immobilization pH could be set in this range. In particular, the immobilization pH was carried out for both linkers at pH 4.5, 7.2 and 8.5. The functionalized wafers were tested for their activity and all values have been compared to a theoretical value. The activated ester showed better results at neutral and basic conditions. The epoxide showed good results at pH 4.5 and 8.5. Additionally, a stability test over seven days was carried out, which showed good results after removing physisorbed enzymes

The results of the WCA and XPS showed lower values as expected which was proposed to originate from a low surface coverage. The FTIR transmission spectroscopy proved to be challenging and should be changed to ATR methods.

Potentially the surface coverage of the linker could be optimized through the reaction with UV source with higher intensity in neat linker solution. Additionally, it could be advantageous to carry out the steps in a Schlenk tube, to avoid oxygen contaminations of the linker solution.

The used processes proved to be a suitable method for immobilization. In turn, the theoretical immobilization for flat silicon surfaces is quite low. For catalytic applications, highly reactive enzymes with good immobilization stability have to be used to gain feasible yields. One approach could be to enlarge the surface area through use of porous silicon.

For the use of sensors, sensitive detection methods have to be developed.

## 5. Experimental Details

### 5.1. Silicon Wafer Specifications:

Supplier:	Silicon Materials	Thickness:	475 - 525 nm
Surface direction:	Si(111)	Diameter:	100 ± 0,5 mm
Dopant:	n-doped / Phosphorus	Resistance:	1 - 10 Ω*cm
Growth method:	Czochralski	Miscut angle $\alpha^0$ :	4°

### 5.2. UV Source:

UV lamp:	GPH303T5L low pressure mercury vapor lamp
Power:	15 W
Radiated power:	4.3 W @ 254 nm.

### 5.3. Water Contact Angle Measurement:

Goniometer:	Küss Easy Drop
Drop size:	1µl
Circle fitting method :	H/W method

### 5.4. FTIR Measurement:

Unit	Bruker VERTEX 70	Reflector speed:	40 kHz
Transmission:	4000-400 cm <sup>-1</sup>	Gas pre-rinse:	400 L/h
Source:	MIR-D316	Gas rinse:	100 L/h.
Beam splitter:	KBr	(during measurement)	
Detector:	MCT		

### 5.5. UV/Vis Measurement:

UV/Vis Spectrometer:	Perkin Elmer Lamda 950 Spectrometer
Lamp (UV):	D2 lamp
Lamp (Vis):	tungsten Lamp
Measurement cell:	Hellma Analytics – quartz SUPRASIL® 10 mm 100-QS

### 5.6. XPS Measurement:

Source:	Specs XRC 1000	Output:	100W
Excitation:	MgK $\alpha$	Measuring spot:	10 x 10 mm <sup>2</sup> Area
Analyzer	Specs Phoibos 150	Vacuum:	10 <sup>-8</sup> mbar

### 5.7. Used Chemicals

Chemical	%	Grade	Supplier	No.
Hydrogen peroxide	30 %	p.a.	Carl Roth	8070.1
Hydrochloric acid	≥ 37 %	p.a.	Sigma-Aldrich	30721
Ammonium hydroxide	33 %		J.T.Baker	6125
Sulfuric acid	≥ 95 %	p.a.	Carl Roth	4623.5
Ammonium fluoride	40 %	s.g.	Sigma-Aldrich	40208
Hydrofluoric acid	50 %	s.g.	Riedel-de-Haen	40276
N-Hydroxysuccinimide	98 %		Sigma-Aldrich	130672
N-(3-Dimethylaminopropyl)- N'-ethylcarbodiimide hydrochloride	≥ 98 %		Sigma-Aldrich	03450
10-Undecenoic acid	98 %		Sigma-Aldrich	124672
1,2-Epoxy-9-decene	96 %		Sigma-Aldrich	410829
Citric acid	≥ 99.5 %	p.a.	Sigma-Aldrich	27488
Ammonium sulfite hydrate	92 %		Sigma-Aldrich	358983
2,6-Dimethoxyphenol	99 %		Sigma-Aldrich	D135550
Dichlormethane	≥ 99.5 %	p.a.	Carl Roth	6053.1
Cyclohexane	99.8 %		VWR Int.	23223.290

p.a. = pro analysi; s.g. = semiconductor grade

Deionized water: TKA Pacific ultra-pure water system  
 $\lambda = 0.065 \mu\text{S cm}^{-1}$  at 25 °C

**References**

- [1] Kumar, R. A.; Clark, D. S.; *Curr. Opin. Chem. Biol.*, 2006, 10, 162–168.
- [2] Zaks, A.; Dodds, D. R.; *Drug Discovery Today*, 1997, 2, 513-531
- [3] Schmid, A.; Dordick, J. S.; Hauer, B.; Kiener, A.; Wubbolts, M.; Witholt, B.; *Nature*, 2001, 409, 258-268
- [4] Battistel, E.; Bianchi, D.; Cesti, P.; Pina, C.; *Biotechnology and Bioengineering*, 1991, 38, 659-664
- [5] Zhang, G.; Huang, M. J.; Luo, Z. H. H.; Tay, G. K. I.; Lim, E. A.; Liu, E. T.; Thomsen, J. S.; *Biosensors and Bioelectronics*, 2010, 26, 365–370
- [6] De Stefano, L.; Rendina, I.; Rossi, A. M.; Rossi, M.; Rotiroli, L.; D’Auria, S.; *J. Phys.: Condens. Matter*, 2007, 19, 395007-395012
- [7] Lorrain, N.; Hiraoui, M.; Guendouz, M.; Haji, L.; *Materials Science and Engineering B*, 176, 2011, 1047–1053
- [8] Rahman, M. A.; Noh, H.; Shim, Y.; *Anal. Chem.*, 2008, 80, 8020–8027
- [9] Levy-Clement, C.; Laboubi, A.; Tenne, R.; Neumann-Spallar, M.; *Electrochimica Acta.*, 1992, 31, 877-888.
- [10] Wong, L.S.; Khan, F.; Micklefield, J.; *Chem. Rev.*, 2009, 109, 4025–4053
- [11] Guiomar, A.; Guthrie, J. T.; Evans, S. D.; *Langmuir*, 1999, 15, 1198-1207
- [12] Kim, J.; Cho, J.; Seidler, P. M.; Kurland, N. E.; Yadavalli, V. K.; *Langmuir*, 2010, 26, 4, 2599–2608
- [13] Qi, C.; Tian, X.; Chen, S.; Yan, J.; Cao, Z.; Tian, K.; Gao, G. F.; Jin, G.; *Biosensors and Bioelectronics*, 2010, 25, 1530–1534
- [14] Aureau, D.; Varin, Y.; Roodenko, K.; Seitz, O.; Pluchery, O.; Chabal, Y. J.; *J. Phys. Chem. C*, 2010, 114, 14180–14186
- [15] Kallio, J. P.; Auer, S.; Jänis, J.; Andberg, M.; Kruus, K.; Rouvinen, J.; Koivula, A.; Hakulinen, N.; *J. Mol. Biol.*, 2009, 392, 895–909
- [16] Lenci, S.; Tedeschi, L.; Pieri, F.; Domenici, C.; *Applied Surface Science*, 2011, 257, 8413–8419
- [17] Subramanian, A.; Kennel, S. J.; Oden, P. I.; Jacobson, K. B.; Woodward, J.; Doktycz, M. J.; *Enzyme and Microbial Technology*, 1999, 24, 26–34
- [18] Lindroos, V.; Tilli, M.; Lehto, A.; Motooka, T.; *Handbook of Silicon Based MEMS Materials and Technologies*, William Andrew, Burlington, 2010
- [19] Hines, M. A.; *Annu. Rev. Phys. Chem.*, 2003, 54, 29–56
- [20] Flidr, J.; Huang, Y.; Newton, T. A.; Hines, M. A.; *J. Chem. Phys.*, 1998, 108, 5542-5553
- [21] Smith, R. K.; Lewis, P. A.; Weiss, P. S. *Prog. Surf. Sci.*, 2004, 75, 1–68.
- [22] Ciampi, S.; Harper, J. B.; Gooding, J. J.; *Chem. Soc. Rev.*, 2010, 39, 2158–2183
- [23] Wojtyk, J. T. C.; Tomietto, M.; Boukherroub, R.; Wayner, D. D. M.; *J. Am. Chem. Soc.* 2001, 123, 1535-1536
- [24] Holleman, F.; Wiberg, E.; Wiberg, N.; *Lehrbuch der Anorganischen Chemie*; 101. Auflage, de Gruyter, 1995
- [25] Bullis, M.W.; In handbook of semiconductor silicon technology; O’mara, W.C.; Herring, R.B.; Hunt, L. P.; 1.ed.; Noyes Publications: New Jersey, 1990, 347-450

- [26] West, A. R.; *Solid State Chemistry and its Applications*, Wiley & Sons, **1984**
- [27] Buriak, J. M.; *Chemical Reviews*, **2002**, 102, 5, 1272-1308
- [28] Kern, W.J. *Electrochem. Soc.*, **1990**, 137, 6, 1887-1892
- [29] Reinhardt, K. A.; Kern, W.; *Handbook of silicon wafer cleaning technology*, 2.ed, William Andrew, Norwich, **2008**
- [30] Kolasinski, K. W.; *Surface Science*, **2009**, 603, 1904–1911
- [31] Monk, D. J.; Soane, D. S.; Howe, R. T.; *Thin Solid Films*, **1993**, 232, 1-12
- [32] Burrows, V. A.; Chabal, Y. J.; Higashi, G. S.; Raghavachari, K.; Christman, S. B.; *Appl. Phys. Lett.*, **1988**, 53, 998-1000
- [33] Higashi, G. S.; Chabal, Y. J.; Trucks, G.W.; Raghavachari, K.; *Appl. Phys. Lett.*, **1990**, 56, 656-658
- [34] Chabal, Y. J.; Higashi, G. S., Raghavachari, K.; *J. Vac. Sci. Technol. A*, **1989**, 7, 2104-2109
- [35] Ling, L.; Kuwabara, S.; Abe, T.; Shimura, F.; *J. Appl. Phys.*, **1993**, 73, 3018-3022
- [36] Neuwald, U.; Hessel, H. E.; Feltz, A.; Memmert, U.; Behm, R. J.; *Appl. Phys. Lett.*; **1992**, 60, 1307-1309
- [37] MacLaren, D. A.; Curson, N. J.; Atkinson, P.; Allison, W.; *Surface Science*, **2001**, 490, 285-295
- [38] Wayner, D. D. M.; Wolkow, R. A.; *J. Chem. Soc., Perkin Trans.*, **2002**, 2, 23–34
- [39] Flidr, J.; Huang, Y.; Hines, M. A.; *J. Chem. Phys.*, **1999**, 6970-6981
- [40] Hessel, H. E.; Feltz, A.; Reiter, M.; Memmert U.; Behm, R. J.; *Chem. Phys. Lett.*, **1991**, 186, 23, 275-280
- [41] Kelly, J. J.; Philipsen, H. G. G.; *Curr. Opinion in Solid State and Materials Science*, **2005**, 84–90
- [42] Hines, M. A.; Chabal, Y. J.; Harris, T. D.; Harris, A. L.; *J. Chem. Phys.*, **1994**, 101, 8055-8072
- [43] Horn, K.; Scheffler, M.; *Handbook of Surface Science*, Vol. 3, **2008**, North Holland, Chapter 16, Kolasinski, K. W., 787-870
- [44] Seidel, H.; Csepregi, L.; Heuberger A.; Baumgärtel, H.; *J. Electrochem. Soc.*, **1990**, 137, 3612-3626
- [45] Ouyang, J. H.; Zhao, X. S.; Li, T.; Zhang, D. C.; *J. Appl. Phys.*, **2003**, 93, 4315-4320
- [46] Volker Lehmann, *Electrochemistry of Silicon: Instrumentation, Science, Materials and Applications*, Wiley-VCH, **2002**
- [47] Wade, C.P.; Chidsey, C.E.D.; *Appl. Phys. Lett.* **1997**, 71, 1697-1681
- [48] Allongue, P.; Kieling, V.; Gerischer, H., *Electrochimica Acta*, **1995**, 40,10, 1353-1360
- [49] Bae, S.; Oh, M.; Min, N.; Paek, S.; Hong, S.; Lee, C. J.; *Bull. Korean Chem. Soc.*, **2004**, 25, 1822-1828
- [50] [http://www.transene.com/elec\\_grade.html](http://www.transene.com/elec_grade.html), 10.03.2012
- [51] Allongue, P.; Henry de Villeneuve, K.; Morin, S.; Boukherroub, R.; Wayner; D.D.M.; *Electrochimica Acta*, **2000**; 45, 4591-4598
- [52] Kato, H.; Taoka, T.; Suto, S.; Nishikata, S.; Sazaki, G.; Nakajima, K.; Yamada, T.; Czajka, R.; Wawro, A.; Kasuya, A.; *e-J. Surf. Sci. Nanotech.*, **2009**, 7, 557-562
- [53] Sieval, A. B.; Van den Hout, B.; Zuilhof, H.; Sudhölter, E. J. R.; *Langmuir*, **2001**, 17, 2172-2181

- [54] Rostovtsev, V. V.; Green, L. G.; Fokin, V. V.; Sharpless, K. B.; *Angew. Chem. Int. Ed.* **2002**, *41*, 2596-2599
- [55] Cicero, R. L.; Chidsey, C. E. D.; Lopinski, G. P.; Wayner, D. D. M.; Wolkow, R. A.; *Langmuir*, **2002**, *18*, 306-307
- [56] Cicero, R. L.; Linford, M. R.; Chidsey, C. E. D.; *Langmuir*, **2000**, *16*, 5688-5695
- [57] Pedone, E.; Li, X.; Koseva, N.; Alpar, O.; Brocchini, S.; *J. Mater. Chem.*, **2003**, *13*, 2825–2837
- [58] Hermanson, G.; *Bioconjugate Techniques*, San Diego, Academic Press, **1996**
- [59] Anjaneyulu, P. S. R., Staros, J. V.; *Int. J. Peptide Protein Res.*, **30**, **1987**, 117-124
- [60] Rusmini, F.; Zhong, Z.; Feijen, J.; *Biomacromolecules*, **2007**, *8*, 1775-1789
- [61] Grazu, V.; Abian, O.; Mateo, C.; Batista-Viera, F.; Fernandez-Lafuente, R.; Guisan, J. M.; *Biomacromolecules* **2003**, *4*, 1495-1501
- [62] Camarero, J. A.; *Peptide Science*, **2007**, *90*, 450 -458
- [63] Saxon, E.; Bertozzi, C.R.; *Science*, **2000**, *287*, 2007-2010
- [64] Köhn, M.; Breinbauer, R.; *Angew. Chem. Int. Ed.*, **2004**, *43*, 3106 –3116
- [65] Moses, J.E.; Moorhouse, A.D.; *Chem. Soc. Rev.*, **2007**, *36*, 1249–1262
- [66] Kalia, J.; Raines, R.T.; *Chem. Bio. Chem.*, **2006**, *7*, 1375–1383
- [67] J. de Graaf, A.; Kooijman, M.; Hennink, W. E.; Mastrobattista, E.; *Bioconjugate Chem.*, **2009**, *20*, 7, 1281-1295.
- [68] Thomas, J. M.; Thomas, W. J.; *Principles and Practice of Heterogeneous Catalysis*, Weinheim, VCH, 1997
- [69] Illanes, A.; *Enzyme Biocatalysis - Principles and Applications*, Springer, **2008**
- [70] [http://www.chemgapedia.de/vsengine/vlu/vsc/de/ch/10/heterogene\\_katalyse/teilschritte\\_der\\_katalyse/teilschritte\\_der\\_katalyse.vlu.html](http://www.chemgapedia.de/vsengine/vlu/vsc/de/ch/10/heterogene_katalyse/teilschritte_der_katalyse/teilschritte_der_katalyse.vlu.html), Hoogestraat, D.; Kuhlmann, A.; Medra, E.; Rößner, F.; Schulz, K.; 04.03.2012
- [71] <http://www.chem.qmul.ac.uk/iubmb/>, IUBMB, Moss, G. P.; 05.03.1012
- [72] Bisswanger, H.; *Enzyme Kinetics - Principles and Methods*, Weinheim, Wiley-VCH, **2002**
- [73] Persichetti, L.; Menditto, R.; Sgarlata, A.; Fanfoni, M.; Balzarotti, A.; *Appl. Phys. Lett.*, **2011**, *99*, 1619071-1619073
- [74] Jakob, P.; Chabal, Y. J.; Raghavachari, K.; Becker, R. S.; Becker, A. J.; *Surface Science*, **1992**, *275*, 407-413
- [75] Voicu, R.; Boukherroub, R.; Bartzoka, V.; Ward, T.; Wojtyk, J.T.C.; Wayner, D.D.M.; *Langmuir*, **2004**, *20*, 11713–11720
- [76] R20 Touahir, L.; Allongue, P.; Aureau, D.; Boukherroub, R.; Chazalviel, J. N.; Galopin, E.; Gouget-Laemmel, A. C.; Henry de Villeneuve, C.; Moraillon, A.; Niedziółka-Jönsson, J.; Ozanam, F., Andresa, J. S.; Sam, S.; Solomon, I.; Szunerits, S.; *Bioelectrochemistry*, **2010**, *80*, 17–25
- [77] [http://www.chem.pku.edu.cn/zshi/gxzy\\_files/Freeze\\_Pump\\_Thaw.pdf](http://www.chem.pku.edu.cn/zshi/gxzy_files/Freeze_Pump_Thaw.pdf), 27.09.2011
- [78] Lichtenegger, G. J.; *Immobilization and Patterning of Organometallic Pd-Catalysts on Si(111) Surfaces via UV-Lithography*, Diploma Thesis, TU Graz, 2011
- [79] <http://webbook.nist.gov/cgi/cbook.cgi?ID=C108883&Mask=400>, 20.04.2012
- [80] Wojtyk, J. T. C.; Morin, K. A.; Boukherroub, R.; Wayner, D. D. M.; *Langmuir*, **2002**, *18*, 6081-6087

## References

---

- [81] Jeanquartier, C.; Schider, G.; Feichtenhofer, S.; Schwab, H.; Schennach, R.; Stettner, J.; Winkler, A.; Gruber-Woelfler, H.; Schitter, G.; Eder, R. J. P.; Khinast, J. G.; *Langmuir*, **2008**, *24*, 13957-13961
- [82] Valeur, E.; Bradley, M.; *Chem. Soc. Rev.*, **2009**, *38*, 606–631
- [83] Zhang, I.; Li, L.; Chen, S.; Jiang, S.; *Langmuir*, **2002**, *18*, 5448-5456
- [84] Morita, M.; Ohmi, T.; Hasegawa, E.; Kawakami, M.; Ohwada, M.; *J. Appl. Phys.*, **1990**, *68*, 1272-1281
- [85] Asanuma, H.; Lopinski, G. P.; Yu, H. Z.; *Langmuir*, **2005**, *21*, 5013-5018
- [86] Liu, Y. J.; Navasero, N. M.; Yu, H. Z.; *Langmuir* **2004**, *20*, 4039-4050
- [87] Perring, M.; Dutta, S.; Arafat, S.; Mitchell, M.; Kenis, P. J. A.; Bowden, N. B.; *Langmuir* **2005**, *21*, 10537-10544
- [88] Böcking, T.; Kilian, K. A.; Gaus, K.; Gooding, J. J.; *Langmuir*, **2006**, *22*, 3494-3496
- [89] Kallio, J. P.; Auer, S.; Jänis, J.; Andberg, M.; Kruus, K.; Rouvinen, J.; Koivula, A.; Hakulinen, N.; *J. Mol. Biol.*, **2009**, *392*, 895–909
- [90] Arafat, A., Daous, M. A.; *Sensors and Actuators B*, **2011**, *152*, 226–234
- [91] Kim, J.; Pike Technologies, [http://www.piketech.com/skin/fashion\\_mosaic\\_blue/application-pdfs/ProbingOrganicSelf-AssembledMonolayersSiliconFTIRSingleReflectanceATR.pdf](http://www.piketech.com/skin/fashion_mosaic_blue/application-pdfs/ProbingOrganicSelf-AssembledMonolayersSiliconFTIRSingleReflectanceATR.pdf) 28.09.2011
- [92] Lummerstorfer, T.; Kattner, J.; Hoffmann, H.; *Anal Bioanal Chem*, **2007**, *388*, 55–64
- [93] Kim, J.; Seidler, P.; Wan, L. S.; Fill, C.; *J. Colloid and Interface Science*, **2009**, *329*, 114–119
- [94] Prasetyo, E. N.; Kudanga, T.; Steiner, W.; Murkovic, M.; Nyanhongo, G. S.; Guebitz, G. M., *Anal Bioanal Chem*, **2009**, *393*, 679–687
- [95] Campos, R.; Kandelbauer, A.; Robra, K. H.; Cavaco-Paulo, A.; Gübitz, G. M.; *Journal of Biotechnology*, **2001**, *89*, 131–139
- [96] Kandelbauer, A.; Maute, O.; Kessler, R. W.; Erlacher, A.; M. Gübitz, G. M.; *Biotechnology and Bioengineering*, **2004**, *87*, 552-563
- [97] <http://www.ebi.ac.uk/ena/data/view/ACC43989>, 02.05.2012
- [98] <http://www.ebi.ac.uk/pdbe-srv/view/entry/3pxl/visualisation.html>, 20.04.2012
- [99] Lin, S. S. J.; Lai, C. M.; Wang, Y. C.; *Food Science and Agricultural Chemistry*, **2000**, *2*, 181-188
- [100] Bonollo, S.; Lanari, D.; Vaccaro, L.; *Eur. J. Org. Chem.*, **2011**, 2587–2598
- [101] Forde, J.; Tully, E.; Vakurov, A.; Gibson, T. D.; Millner, P.; Ó'Fágáin, C.; *Enzyme and Microbial Technology*, **2010**, *46*, 430–437
- [102] Dagys, M.; Haberska, K.; Shleev, S.; Arnebrant, T.; Kulys, J.; Ruzgas, T.; *Electrochemistry Communications*, **2010**, *12*, 933–935
- [103] Buchholz, K.; Kasche, V.; Bornscheuer, U.T.; *Biocatalysts and Enzym Technology*, Weinheim, Wiley-VCH, **2005**
- [104] [http://www.tascon.eu/media/de/Praxis/Analysetechniken/XPS\\_de.pdf](http://www.tascon.eu/media/de/Praxis/Analysetechniken/XPS_de.pdf), 01.05.2012
- [105] <http://www.rcsb.org/pdb/explore/explore.do?structureId=3FPX2>, 20.04.2012
- [106] Grabarek, Z.; Gergely, J.; *Analytical Biochemistry*, **1990**, *185*, 131-135